

Received 27 February 2024, accepted 24 March 2024, date of publication 9 April 2024, date of current version 23 April 2024.

Digital Object Identifier 10.1109/ACCESS.2024.3386560

## RESEARCH ARTICLE

# Multi-Objective Water Strider Algorithm for Complex Structural Optimization: A Comprehensive Performance Analysis

KANAK KALITA<sup>1,2</sup>, NARAYANAN GANESH<sup>3</sup>, RC NARAYANAN<sup>4</sup>,  
PRADEEP JANGIR<sup>5</sup>, DIEGO OLIVA<sup>6</sup>, (Senior Member, IEEE),  
AND MARCO PÉREZ-CISNEROS<sup>6</sup>, (Senior Member, IEEE)

<sup>1</sup>Department of Mechanical Engineering, Vel Tech Rangarajan Dr. Sagunthala Research and Development Institute of Science and Technology, Avadi, Chennai 600062, India

<sup>2</sup>University Centre for Research and Development, Chandigarh University, Mohali 140413, India

<sup>3</sup>School of Computer Science and Engineering, Vellore Institute of Technology, Chennai 600127, India

<sup>4</sup>Department of Computer Science and Engineering, Sona College of Technology, Salem 636005, India

<sup>5</sup>Department of Biosciences, Saveetha School of Engineering, Saveetha Institute of Medical and Technical Sciences, Chennai 602105, India

<sup>6</sup>Departamento de Ingeniería Electro-Fotónica, Centro Universitario de Ciencias Exactas e Ingenierías (CUCEI), Universidad de Guadalajara, Guadalajara, Jalisco 44430, Mexico

Corresponding authors: Diego Oliva (diego.oliva@cucei.udg.mx) and Marco Pérez-Cisneros (marco.perez@cucei.udg.mx)

**ABSTRACT** For various daunting physical world structural optimization design problems, a novel multi-objective water strider algorithm (MOWSA) is proposed, and its non-dominated sorting (NDS) framework is explored. This effort is inspired by the recent proposals for the Water Strider Algorithm, a population-based mathematical paradigm focused on the lifespan of water strider insects. The crowding distance characteristic is integrated into MOWSA to improve the exploration and exploitation trade-off behavior during the advancement of the quest. Furthermore, the suggested a posteriori approach exercises the NDS technique to maintain population diversity, a key issue in meta-heuristics, especially for multi-objective optimization. Structural mass reduction and nodal deflection maximization are two diverse objectives for the posed design problems. At the same time, stress on the components and discrete cross-sectional areas are imposed on safety and side constraints, respectively. Eight planar and spatial truss design problems demonstrate the utility of the proposed MOWSA approach for solving complex problems where the performance analysis is based on ten globally accepted metrics. Moreover, MOWSA outcomes were compared with four state-of-the-art optimization techniques to measure the viability of the suggested algorithm. MOWSA outperforms other considered algorithms concerning computational run to achieve optimal solutions and their qualitative behavior over Pareto fronts. The Matlab code for MOWSA can be obtained from <https://github.com/kanak02/MOWSA>.

**INDEX TERMS** Multi-objective, truss design, computational analysis, exploitation, exploration, constraints techniques.

## I. INTRODUCTION

In many real-world challenging problems with diverse frameworks, meta-heuristics (MHs) have been successfully implemented. MHs are powerful and robust gradient-free stochastic optimization methods for solving various numerical and

The associate editor coordinating the review of this manuscript and approving it for publication was Daniel Augusto Ribeiro Chaves<sup>1</sup>.

combinatorial optimization problems. Typically, MHs are adapted for complex functions such as discrete, multimodal, non-linear, noisy, and non-gradient, which cause computation costs and consumption of a high amount of time. Besides, occasionally, for such problems, it is impossible to get solutions [1], [2]. Due to their unique, effective mechanisms and tools in recent years, MHs have moved into the limelight, making them popular techniques for solving

various real-world intricate problems [3]. With background, traditional mathematics methods either fail to answer these complex design functions or consume more computational time. They require gradient derivatives calculation, which would make it difficult to solve significant problems. Some competing techniques to solve these optimization problems are exact solution methods like linear or nonlinear programming, a branch, and a bound method, among others. But they require quite a bit of computation time to solve such a large problem [4], [5], and [6]. Moreover, inaccurate gradient information can lead them to the wrong solutions.

Engineering design issues comprised of multi-objective (MO) structure optimization are usually associated with diverse objectives such as weight minimization and maximum nodal deflection [7]. To address such challenging MO problems, MHs have demonstrated their outstanding performance in recent years. Some of the renowned MHs are Genetic Algorithm (GA) [8], Simulated Annealing (SA) [9], Differential Evolution (DE) [10], Particle Swarm Optimization (PSO) [11], Artificial Bee Colony (ABC) [12], Ant Colony Optimization (ACO) [13], Tabu Search (TS) [14], Heat Transfer Search Algorithm (HTS) [15], a Cuckoo Search Algorithm [16], Non-dominated Sorting Genetic Algorithm (NSGA-II) [17], Strength Pareto Evolutionary Algorithm (SPEA2) [18], a Pareto Envelope-based Selection Algorithm (PESA-II) [19], and a Pareto Archive Evolution Strategy (PAES) [20]. While the outcomes generated by MHs are regarded as approximate optimal results, they can be accomplished in a reasonable time [21]. Gandomi and Alavi cited that MHs are more powerful than the traditional methods typically used to address complex issues [22]. MHs were widely enforced to various real problems owing to their adequate performance and convenience of implementation [23], [24]. In recent decades, MHs have become astonishingly prevalent due to ease, versatility, derivative-free frameworks, and local optimum escape [2], [15], [21].

One of the most significant drawbacks of such algorithms, like GA and SA, is that they reported a slow convergence rate, which results in higher computational effort. Another flaw is the possibility of the results being trapped in an optimal local region, as seen in PSO, TS, ACO, and HS. Another crucial aspect of an efficient optimization technique is the potential to establish a good trade-off amid global diversification and local intensification of search space [25]. This is critical because the former aids in quickly finding high-quality solution locations in the quest field. At the same time, the latter contributes to hunting regions that are either previously exposed or may not provide better solutions in a short amount of time [26]. To address these limitations, several novel MHs have been developed so far, such as Salp Swarm [27], modified symbiotic organism search [28], Moth Flame [29], modified HTS [30], Grasshopper optimization [31], improved HTS [32], Marine Predators [33], Grey Wolf [31], ant lion [34], enhanced chaotic JAYA [35], and many more.

Nevertheless, an MH algorithm cannot answer every function efficiently as per the 'No Free Lunch' hypothesis [36]. An MH may offer a greater outcome in a certain design problem, but a similar approach might cause a weak outcome in different test functions. Simply put, no MH offers the best answer for every problem. For example, Hertz and de Werra [37] claimed that TS in the graph coloring problem is more excellent than SA. In contrast, SA is better than TS in the lot-sizing problem, as per Kuik et al. [38]. However, Lee and Kim [39] described that TS and SA were equally efficient in a project scheduling problem. Furthermore, Yang [40] argued that there is no accepted method for contrasting the performance of different MHs. Consequently, discovering new, more powerful MHs is an active subject [41].

The primary focus of truss optimization research has been achieving optimal single-objective truss design. This typically involves reducing structural weight or mass while adhering to stress, displacement, or frequency constraints. Numerous metaheuristic approaches have been explored for this type of design challenge. For instance, Kaveh and Talatahari [42] applied the imperialist competitive algorithm to optimize skeletal structures, demonstrating its effectiveness with two space trusses and two frame structures. Kaveh and Mahdavi [43] formulated the colliding bodies optimization algorithm for benchmark truss structure optimization. Mortazavi et al. [44] developed a PSO variant with a fly-back mechanism and a weight particle concept for truss structure sizing and layout, proving competitive with other advanced metaheuristic algorithms. Farshchin et al. [45] introduced a multi-class teaching-learning-based optimization for shape and sizing optimization of truss structures, considering multiple natural frequency constraints. Degertekin et al. [46] utilized the parameter-free Jaya algorithm for minimizing the weight of truss structures under natural frequency constraints. However, these algorithms might underperform in multi-objective optimization scenarios due to their need for a balanced approach to exploration and exploitation.

In contrast, multi-objective truss optimization has seen less development, primarily due to the complexity of conflicting objectives, nonlinear constraints, multi-modality, and non-convex feasible regions [47]. Despite this, multi-objective optimization is more prevalent in real-world scenarios, offering the advantage of handling multiple objectives for decision-making. The choice of an algorithm in multi-objective truss optimization significantly influences the outcomes.

A significant portion of this research is dedicated to Pareto-based algorithms. Coello and Christiansen [48] introduced a genetic algorithm tailored for multi-objective truss optimization. In another study [49], a PSO variant, dubbed FC-MOPSO, was enhanced to preserve diversity and achieve Pareto solutions in truss optimization tasks. The development of a modified symbiotic organism search (MOSOS), tested on five distinct truss design problems, is documented in [50]. Kaveh and Mahdavi [51] presented a multi-objective colliding bodies optimization algorithm

for structural design, demonstrating superior Pareto fronts compared to NSGA-II and MOPSO across various structures, including a 120-bar truss dome and a 582-bar tower truss. Kumar et al. [2] explored the efficacy of the multi-objective passing vehicle search (MOPVS) in structural design, noting its proficiency in generating optimal Pareto fronts. Tejani et al. [15] devised a multi-objective heat transfer search algorithm (MOHTS) for structural design, validated through five truss optimization scenarios. Subsequently, a modified version of this algorithm was also developed for structural design challenges [30]. Premkumar et al. [52] proposed a multi-objective gradient-based optimizer (MOGBO) showing promising results in various truss optimization problems, including those involving 10 to 942 bars. Further advancements in this field include innovative MOPVS [53], multiobjective forensic-based investigation algorithms [54], multiobjective thermal exchange optimization algorithms [55], and decomposition-based multi-objective heat transfer search [56]. Although these algorithms generally yield satisfactory Pareto solutions, stability in different measure indices like hypervolume and inverted generational distance can vary.

Beyond these developments, research has also delved into differential evolution variants for multi-objective truss optimization. Vargas et al. [57] examined generalized differential evolution (GDE) and its variations for truss optimization with dual objectives of total weight and structural displacement, achieving impressive Pareto fronts. Carvalho et al. [58] assessed different differential evolution algorithms for three-objective truss optimization, affirming their applicability in complex scenarios. Lemonge et al. [3] innovated the third evolution phase of GDE (GDE3) with an adaptive penalty method for frequency-constrained truss optimization. Anosri et al. [59] proposed iSHAMODE, a SHAMODE variation, to address truss optimization with dual objectives of total weight and reliability index, surpassing other algorithms in hypervolume statistical values.

Recently, Kaveh and Eslamlou [60] proposed a new nature-based MH called the water strider algorithm (WSA) that mimics the water strider insect life cycle behavior. These insects' territorial behavior, mating way, ripple communication, foraging, and succession characteristics are converted into a simplified mathematical framework. The authors investigated the exploitative, exploratory, local trap escaping, convergence behavior of WSA through its applications in various design problems and found it efficient and straightforward. However, the authors suggested further improvement and investigation for MO large-scale real-world problems.

This study introduces a novel Non-Dominated Sorting (NDS)-based Multi-Objective Water Strider Algorithm (MOWSA), innovatively combining the NDS framework [17], [61] with the fundamental principles of the Water Strider Algorithm (WSA). The proposed MOWSA model showcases several key contributions to the field of optimization:

- The study presents a unique approach by integrating Non-Dominated Sorting (NDS) with the Water Strider Algorithm (WSA), enhancing its capability to address complex multi-objective optimization problems.
- MOWSA employs a crowding distance mechanism, crucial for maintaining diversity in solutions. This feature prevents solution clustering and promotes comprehensive search space exploration while focusing on high-quality, non-dominated solutions.
- The algorithm is designed to balance exploration and exploitation, which is crucial for effective optimization. In its early iterations, MOWSA emphasizes discovering new solutions (exploration), while in later stages, it focuses on refining and converging towards optimal solutions (exploitation), guided by continuous assessment through NDS.
- The efficacy of MOWSA is thoroughly tested across a range of structural design problems, including eight (10-, 25-, 37-, 60-, 72-, 120-, 200-, and 942-bar) diverse truss bar and (LSMOP1-LSMOP9) benchmark problems [62], demonstrating its versatility and robustness.
- MOWSA's performance is rigorously assessed both quantitatively and qualitatively, in comparison with other notable multi-objective optimization algorithms such as MO Heat Transfer Search (MOHTS) [15], NDS Grey Wolf Optimizer (NSGWO) [61], MO Colliding Bodies Optimization (MOCBO) [51], NSGA-II, and MO Multi-Verse Optimizer (MOMVO) [63].

The rest of the paper is structured as follows: Section II elucidates the underlying principles of the basic WSA optimizer. Section III delineates the proposed NDS-based MOWSA algorithm and its operational mechanics. Section IV discusses the multi-objective design optimization mathematical framework. Section V delves into a detailed analysis of performance and results from the truss bar problem evaluations. Finally, Section VI presents conclusions from the study, future research prospects, and potential applications.

## II. FUNDAMENTAL WATER STRIDER ALGORITHM

Kaveh and Eslamlou proposed a new population-based meta-heuristic algorithm called a Water Strider Algorithm (WSA) [60]. The WSA algorithm has five pivotal stages: inception, territorial formation, mating, feeding, and death. The algorithm conceptualizes the search space as a lake, where diverse territories represent potential solutions, and the objective function is metaphorically akin to food sources. The optimization challenges addressed here are framed as minimization problems, implying that a lower objective value equals a more favorable solution. All significant steps for the WSA are outlined below.

### Step 1 (Birth Inception):

The genesis of water striders (WSs) is modeled as the hatching of eggs scattered across the lake, formulated as Eq. 1.

$$WS_i^0 = Ub + rand \times (Ub - Lb), i = 1, 2, \dots, nws \quad (1)$$

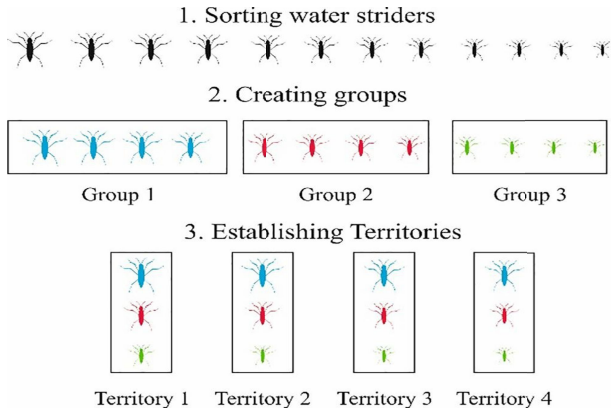


FIGURE 1. Visual representation of creating groups and territory establishment.

Here,  $WS_i^0$  signifies the initial locale of the  $i^{th}$  water strider.  $Ub$  and  $Lb$  represent the upper and lower limits, indicating the maximum and minimum permissible values;  $rand$  is a random value between 0 and 1;  $nws$  denotes the total count of WSs. The preliminary positions of the WSs are evaluated via an objective function to ascertain their fitness within the lake.

Step 2 (Territorial Formation):

Building on the concepts introduced in Step 1, As illustrated in Fig. 1, WSs establish territories for dwelling, mating, and foraging. To form ( $nt$ ) territories, the WSs are organized based on their fitness and divided into orderly groups of ( $nws/nt$ ). Each group's  $j^{th}$  member is allocated to the  $j^{th}$  territory ( $j = 1, 2, \dots, nt$ ), ensuring an equal distribution of WSs in each territory. As highlighted in Step 4, the females typically occupy the most advantageous positions (optimal foraging habitats) within each territory, denoted by the highest and lowest fitness locations as female (optimal) and male (keystone) positions, respectively.

Step 3 (Mating Process):

Mating is a pivotal aspect of the lifecycle of water striders. As previously mentioned, the males initiate courtship with ripples, eliciting responses from females in the form of attractive or repulsive signals. The likelihood of an attractive response is set at  $p$ , leaving a  $(1-p)$  chance for a repulsive response. For simplification,  $p$  is assumed to be 50%. If a female responds positively, they converge and mate. This is depicted in Fig. 2.a, with the post-mating position illustrated in Fig. 2.b. Conversely, as described in Step 3, a female's rejection leads to a series of interactions depicted in Fig. 2.c. Following these interactions, the new position of the keystone is determined by Eq. (2a):

$$\begin{cases} WS_i^{t+1} = WS_i^t + R.rand \\ \text{if mating happens probability } (pm)(p < pm = 0.5), \\ WS_i^{t+1} = WS_i^t + R.(1 + rand) \\ \text{otherwise} \end{cases} \quad (2a)$$

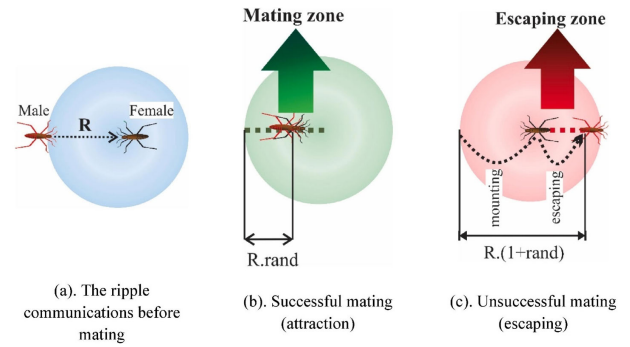


FIGURE 2. Depiction of water striders' mating rituals and their subsequent location shifts.

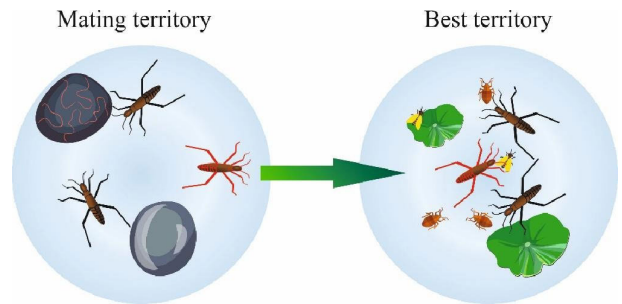


FIGURE 3. Illustration of the foraging activities undertaken by water striders when insufficient food is located at a new site post-mating.

The position  $WS_i^t$  represents the  $i^{th}$  WS's locale in the  $t^{th}$  cycle, with  $rand$  and  $R$  retaining their previously defined meanings. The selection of the female WS is based on a fitness proportionate mechanism, such as roulette wheel selection. The length of  $R$  equates to the Euclidean distance between the male ( $WS_i^{t-1}$ ) and female WSs ( $WS_F^{t-1}$ ), as shown in Eq. (2b) and Fig. 2.

$$R = WS_F^{t-1} - WS_i^{t-1} \quad (2b)$$

Step 4 (Feeding):

Following mating, regardless of its outcome, WSs expend significant energy. Hence, they forage for sustenance in their new positions. The objective function's value gauges food availability. If the new value surpasses the previous, it indicates successful foraging. Otherwise, the WS moves towards the territory with the highest fitness, guided by Equation 3 to a locale near the best WS of the lake ( $WS_{BL}^t$ ), as illustrated in Fig. 3.

$$WS_i^{t+1} = WS_i^t + 2 \times rand \times (WS_{BL}^t - WS_i^t) \quad (3)$$

It should be mentioned that the inability to improve the previous cost value is interpreted as a metaphor for the condition  $2 * rand$  used.

Step 5 (Death and Succession):

The outcome of the foraging effort is assessed by comparing the new fitness value with the previous. If the new value is lower, it signifies the WS's demise due to unsuccessful foraging and increased territorial conflict risk. In this scenario, a newly matured larva assumes the



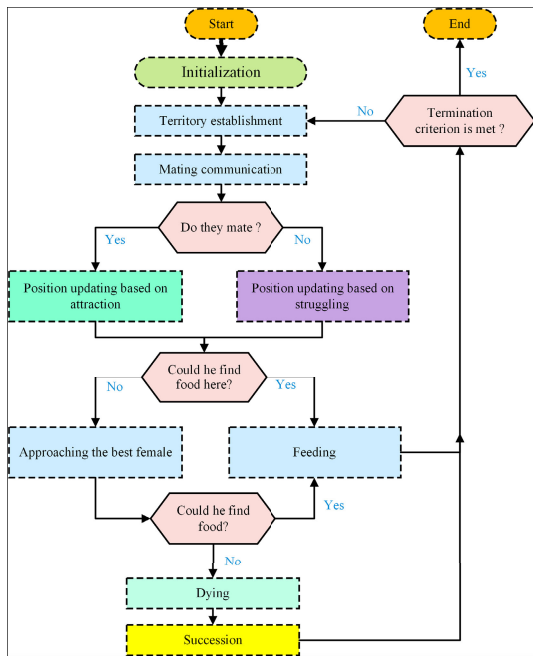


FIGURE 4. Flowchart of the WSA.

deceased’s role as the keystone. The successor’s position is randomly initialized within the territory as per Eq. 4.

$$WS_i^{t+1} = Lb_j^t + 2 \times rand \times (Ub_j^t - Lb_j^t) \quad (4)$$

where  $Ub_j^t$  and  $Lb_j^t$  define the territorial boundaries of the deceased WS.

Step 6 (WSA Termination):

Suppose the termination criteria do not return the MH loop to the mating step. In this case, the termination condition is the maximum iteration count ( $MaxIter$ ). WSA flowchart is shown in Fig. 4.

### III. MULTI-OBJECTIVE WATER STRIDER ALGORITHM

The proposed multi-objective water strider algorithm (MOWSA) optimizer employs an elitist non-dominated sorting (NDS) approach and the crowding distance (CD) mechanism to maintain diversity [63]. This process begins with an elitist, non-dominated sorting to differentiate between various non-domination levels. Then it utilizes the crowding distance method to ensure diversity within the optimal solution set.

Initially, every solution obtained from the basic WSA search or a randomly generated initial population  $P_0$  is evaluated against all objectives in the objective function values and non-dominated solutions (NDS) being found. Additionally, a domination count  $n_p$  (indicating the number of solutions that dominate a particular solution p) and a set of solutions  $S_p$  dominated by p are determined. In the next step, all solutions p are assigned a domination count of zero and classified into the first non-dominated level, the Pareto Front (PF), with their non-domination rank ( $NDR_p$ ) set to 1. Then, for each solution p with a non-zero domination count, the domination count of each member q in  $S_p$  its dominated

### Algorithm 1 Pseudocode for MOWSA

- Step 1: Initially generate population ( $P_0$ ) randomly in solution space (S).
- Step 2: Evaluate objective space (F) for the generated population ( $P_0$ ).
- Step 3: Sort based on the elitist non-dominated sort method and find the non-dominated rank (NDR) and fronts.
- Step 4: Compute crowding distance (CD) for each front.
- Step 5: Update solutions ( $P_j$ )
- Step 6: Merge  $P_0$  and  $P_j$  to create  $P_i = P_0 \cup P_j$ .
- Step 7: For  $P_i$  perform Step 2.
- Step 8: Based on NDR and CD sort  $P_i$ .
- Step 9: Replace  $P_0$  with  $P_i$  for  $N_p$  first members of  $P_i$ .

set  $n_q$  is decreased by one. If a solution q count drops to zero, it’s placed in the second non-domination level  $NDR_q$  and assigned a rank of 2. This process is repeated for each member of the second non-domination level to form the third level, and so on, until the entire population is sorted into different non-domination levels. Then, the WSA reproduction with Eqs. 2a - 4 is employed to generate the new positions of the striders where WS is selected from those non-dominated solutions. The survivors of the next generation are those sorted from the combination of the old and new positions of the striders, who apply the crowding distance mechanism. In the crowding distance approach, the population is first sorted based on the value of each objective function in ascending order. The boundary solutions ( $i = 1$  and  $i = l$ , where  $l$  is the total number of solutions in a particular non-dominated set) are assigned an infinite crowding distance. For the remaining solutions in the sorted population ( $i = 2$  to  $i = l - 1$ ), the crowding distance for each objective  $j$  ( $j = 1, 2 \dots m$ ) is calculated based on the difference in the objective function  $j$  values between its neighboring solutions ( $i + 1$  and  $i - 1$ ).

$$CD_j^i = \frac{fobj_j^{i+1} - fobj_j^{i-1}}{fobj_j^{max} - fobj_j^{min}} \quad (5)$$

From 5  $fobj_j^{max}$  and  $fobj_j^{min}$  are the maximum and minimum values of  $j^{th}$  objective function. After assigning crowding distances to all solutions in a non-dominated set, each solution  $i$  is characterized by two attributes: its non-domination rank  $NDR_i$  and its crowding distance  $CD_i$ . A crowded comparison operator ( $<_n$ ) is used to select between two solutions ( $i$  and  $j$ ),  $i <_n j$  preferring the one with the lower non-domination rank ( $NDR_i < NDR_j$ ), or in case of a tie ( $NDR_i = NDR_j$ ), the one with the higher crowding distance ( $CD_i > CD_j$ ).

Algorithm 1 shows The MOWSA algorithm’s pseudo-code. The algorithm begins by defining the necessary parameters, like a population size ( $N_p$ ), termination criteria, and the max iterations ( $MaxIter$ ) to run MOWSA. Then, in the feasible search space region S, a set of randomly generated water striders’ positions  $P_0$  is formed, and each objective function in space vector ‘F’ for ‘ $P_0$ ’ is evaluated. Finally,

Po is subjected to the elitist-based CD and NDS. Fourth, a new  $P_j$  population is created, then combined to  $P_0$  to form a new population  $P_i$ . This  $P_i$  has been sorted as per elitist NDS and CD and NDR data. To create a new set of water striders' positions for the next generation, the best  $N_p$  solutions are evaluated. Finally, until the termination criteria are met, the procedure is repeated.

**A. BEST COMPROMISE SOLUTION (BCS) AS PER FUZZY DECISION**

The BSC used to find the best compromise solution among all solutions obtained in the Pareto front, which Fuzzy Decision governs, is adopted to find the best fitness for each of the objective functions as per [64], [65] and functions  $\mu_i^j$  defined as follows:

$$\mu_i^j = \begin{cases} 1, & \text{if } f_i^j \leq f_{min}^j \\ \frac{f_{max}^j - f_i^j}{f_{max}^j - f_{min}^j}, & \text{if } f_{min}^j \leq f_i^j \leq f_{max}^j \\ 0, & \text{if } f_i^j \geq f_{max}^j \end{cases} \tag{6}$$

$$\mu(Normalized) = \frac{\sum_{j=1}^{N_{obj}} \mu_{ij}}{\sum_{i=1}^M \sum_{j=1}^{N_{obj}} \mu_{ij}} \tag{7}$$

where  $M$  is the number of NDS,  $N_{obj}$  is the number of the objective functions, and  $f_{max}^j$  and  $f_{min}^j$  are the respective objective function's max and min values. The value with the highest value of compromise has the highest value of  $\mu_i$ .

**B. CONSTRAINT HANDLING APPROACH**

MOWSA employs a static penalty, as shown below:

$$f_j(X) = f_j(X) + \sum_{i=1}^p p_i \max\{g_i(X), 0\} + \sum_{i=p}^{NC} p_i \max\{|h_i(X)| - \delta, 0\} \tag{8}$$

where  $f_j(X)$ ;  $j = 1, 2, \dots, n$  is the objective function,  $X = x_1, x_2, \dots, x_m$  are design variables,  $g_i(X) \leq 0$ ,  $i = 1, 2, \dots, p$  are inequality constraints,  $h_i(X) = 0$ ;  $i = p + 1, \dots, NC$  and  $\delta$  are equality and tolerance inequality constraints.

**C. COMPUTATION COMPLEXITY OF MOWSA**

The computation complexity (CC) of MOWSA adopted from NSGA-II, similar to the MOHTS [15], NSGWO [61], MOCBO [51] and MOMVO [63] and [64]. The complexity =  $O(dim \times N_p + Cost(f_{obj}) \times N_p)$  for the first iteration. The computational time complexity =  $O(dim \times N_p + Cost(f_{obj}) \times N_p) + (NDS + CD) \times dim$  afterwards. The overall time complexity  $Max_{it}$  to time =  $O(M) | M = O(dim \times Max_{it} \times N_p + Cost(f_{obj}) \times Max_{it} \times N_p) + (NDS + CD) \times Max_{it} \times dim + (NDS + CD) \times Max_{it} \times Cost(f_{obj})$ .

**IV. THE DESIGN PROBLEMS**

Optimizing the design of trusses in a multi-objective context presents a significant challenge, mainly due to the competing nature of objectives, complex constraints, and the discrete nature of design variables, specifically in terms of cross-sectional areas. This study focuses on optimizing truss structures with dual objectives: reducing the overall weight and compliance while adhering to permissible stress limits. Achieving an optimal balance between these divergent objectives is inherently difficult, as optimizing one often compromises the other. Moreover, the nonlinear constraints imposed on stress further complicate the optimization process by restricting the range of viable design variables. Unlike single-objective optimization, the goal here is not to pinpoint a singular optimal solution but to identify a set of Pareto optimal solutions, each representing a different trade-off between the objectives. The MO structural optimization problem considers structure weight minimization and maximization of nodal deflection as objective functions. The mathematical model is as follows:

Find,

$$A = A_1, A_2, \dots, A_m \tag{9}$$

to minimize the truss mass:  $f_1(A) = \sum_{i=1}^m A_i \rho_i L_i$  and maximize nodal deflection:  $f_2(A) = \max(|\delta_j|)$

Subject to:

Behaviour constraints:

Stress constraints,  $g(A) = |\sigma_i| - \sigma_i^{max} \leq 0$

Side constraints:

Cross-sectional area constraints  $A_i^{min} \leq A_i \leq A_i^{max}$

where,  $i = 1, 2, \dots, m$ ;  $j = 1, 2, \dots, n$ .  $A_i$  presents a design variable vector;  $\rho_i$  and  $L_i$  are the weight density and bar length, respectively;  $E_i$  and  $\sigma_i$  show Young's Modulus and permissible stress of ' $i^{th}$ ' bar, respectively. The permissible upper and lower limits are signified by superscripts ' $max$ ' and ' $min$ ', respectively. All variables' details are represented in Table 1.

**V. EMPIRICAL EVALUATION**

To inspect the coverage, convergence, exploration, and exploitation of MOWSA, large 2-D and 3-D trusses were tested and compared with other distinguished MO methods present in the literature as the MOHTS [15], NSGWO [61], MOCBO [51] and MOMVO [63]. The subsequent section explains the nine large-scale multiobjective benchmark problems (LSMOP1-LSMOP9) with 300 decision variables and eight problems, i.e., planar 10-bar, spatial 25-bar, 60-bar ring, 72-bar, dome 120-bar, 200-bar, and tower 942-bar truss design that were measured [2], [30]. Table 1 shows design considerations and other properties assumed to optimize eight trusses. Also, Figures 5, 8, 11, 14, 17, 20, 23, and 26 illustrate load directions, constraints, and dimensions.

TABLE 1. Design considerations of the truss problems.

Truss bar problems	Design variables	Loading conditions (N)	Constraints (Pa)	Density (kg/in <sup>3</sup> )	Young Modulus (Pa)	Cross Section Area (A <sup>min</sup> , A <sup>max</sup> )
10 bar	10	$P_{y2} = P_{y4} = -10^5$	$\sigma_{max} = 4 * 10^8$	$\rho = 7850$	$E = 2 * 10^{11}$	$A^{min} = zeros(10, 1)$ $A^{max} = 41 * ones(10, 1)$
25 bar	8	$P_{x1} = 10^4; P_{y1} = P_{y2} = P_{z1} = P_{z2} = -10^5;$ $P_{x3} = 5 * 10^4; P_{x6} = 6 * 10^4;$				$A^{min} = zeros(8, 1)$ $A^{max} = 41 * ones(8, 1)$
37 bar	15	—				$A^{min} = zeros(15, 1)$ $A^{max} = 41 * ones(15, 1)$
60 bar	25	Case 1 : $P_{x1} = -10^5; P_{x7} = 9 * 10^5;$ Case 2: $P_{x15} = P_{x18} = -8 * 10^5;$ $P_{y15} = P_{y18} = 3 * 10^5;$ Case 3: $P_{x22} = -20 * 10^5; P_{y22} = 10^5;$				$A^{min} = zeros(25, 1)$ $A^{max} = 41 * ones(25, 1)$
72 bar	16	Case 1: $P_{x1} = P_{y1} = 2 * 10^6; P_{z1} = -2 * 10^6;$ Case 2: $P_{z1} = P_{z2} = P_{z3} = P_{z4} = -2 * 10^6;$				$A^{min} = zeros(16, 1)$ $A^{max} = 41 * ones(16, 1)$
120 bar	7	—				$A^{min} = zeros(7, 1)$ $A^{max} = 41 * ones(7, 1)$
200 bar	29	—				$A^{min} = zeros(29, 1)$ $A^{max} = 41 * ones(29, 1)$
942 bar	59	At each node: Vertical loading: Section 1: $P_z = -6 * 10^3;$ Section 2 : $P_z = -12 * 10^3;$ Section 3 : $P_z = -18 * 10^3;$ Lateral loading: Right-hand side: $P_x = 3 * 10^3;$ Left-hand side: $P_x = 2 * 10^3;$ Lateral Loading: $P_y = 2 * 10^3;$				$A^{min} = zeros(59, 1)$ $A^{max} = 41 * ones(59, 1)$

A. PERFORMANCE EVALUATION

In this paper, all MHs are performed 30 times independently for all problems. Population size and maximum iteration numbers are 40 and 500, respectively [65].

- The Hypervolume (HV) and Inverted-Generational Difference (IGD) are taken to test the uniformity, convergence simultaneously, and spread of NDS obtained from the computation test. The higher HV, the better the Pareto front, whereas the lower IGD, the better the Pareto front.
- To test the search efficiency and reliability of the MHs as quicker convergence rate Generational Distance (GD), Spread (SD), Coverage (CVG), and Coverage over Pareto Front (CPF) are taken [66] and [67].
- To test the computational complexity, Runtime (RT) metric and for combined diversity-spread, spacing (SP), Diversity (DM), and Pure Diversity (PD) metrics are performed [65], [66], and [67]. The lower (i.e. GD, CVG, SP, SD, IGD, and RT) and higher (i.e. CPF, DM, PD, and HV) indicators result represent the better optimal front.
- The mean and standard deviation (STD) values of the metrics are observed as the statistical performer yardstick [2] and [3].
- Friedman’s rank test (FNRT) is considered as a statistical test of all MHs [15] and [24].

$$GD = \frac{\sqrt{\sum_{i=1}^{no} d_i^2}}{n} \tag{10}$$

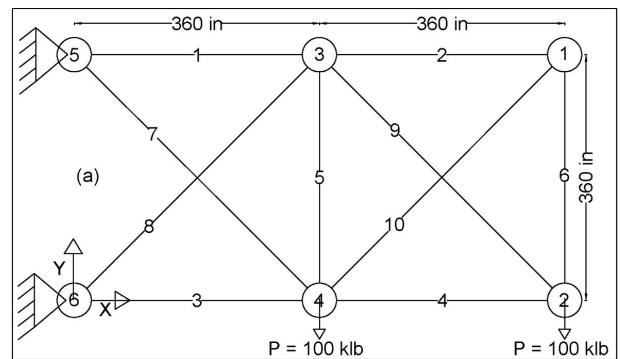


FIGURE 5. The 10-bar truss.

$$IGD = \frac{\sqrt{\sum_{i=1}^n (d'_i)^2}}{n} \tag{11}$$

$$SP \triangleq \sqrt{\frac{1}{n-1} \sum_{i=1}^n (\bar{d} - d_i)^2} \tag{12}$$

$$SD = \sqrt{\sum_{i=1}^0 \max(d(a_i, b_i))} \tag{13}$$

$$PD = \frac{\sum_{H(i,j,...) \neq 0} m(h(i, j, \dots))}{\sum_{H(i,j,...) \neq 0} m(H(i, j, \dots))} \tag{14}$$

$$HV = \Lambda \left( \bigcup_{s \in PF} \{s' | s < s' < s^{nadir}\} \right) \tag{15}$$

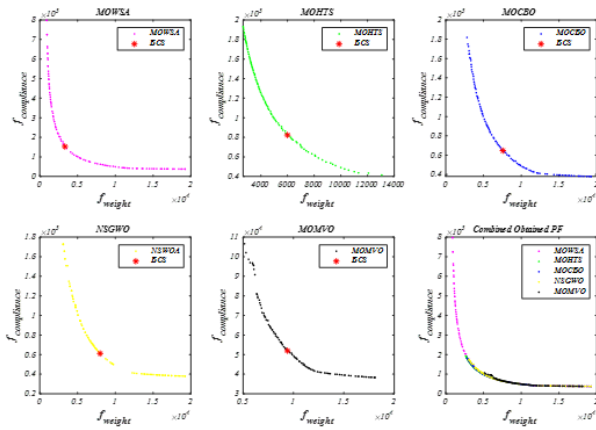


FIGURE 6. Best pareto fronts of considered algorithms for 10-bar truss.

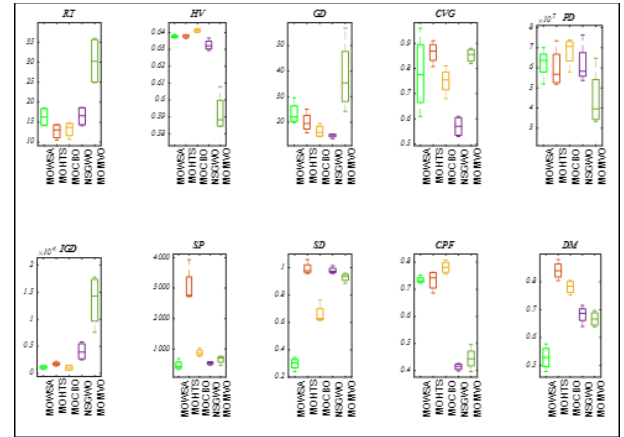


FIGURE 7. Box plots of considered algorithms for 10-bar truss.

$$DM = \frac{d_f + d_l + \sum_{i=1}^{N-1} |d_i - \bar{d}|}{d_f + d_l + (N - 1)\bar{d}} \quad (16)$$

$$CVG = \frac{\sum_{i=1}^n \psi_i}{N},$$

$$\psi_i = \begin{cases} 1, & \text{if } P_i \in PF \text{ and } \alpha_{i-1} \leq \tan \frac{f_1(x)}{f_2(x)} \leq \alpha_n \\ 0, & \text{Otherwise} \end{cases} \quad (17)$$

$$CPF = \frac{\sum_{i=1}^n PF_i}{N} \quad (18)$$

$$RT = \frac{\sum_{i=1}^n T_i}{n}. \quad (19)$$

where ‘no’ is the True Pareto solution (PS) number, ‘nt’ is the true Pareto optimal solutions number, ‘o’ is the number of the objectives,  $\bar{d}$  is the mean of all  $d_i$ ,  $d_i$ , and  $d'_i$  specifies the Euclidean distance,  $n$  is PS number,  $d_i = \min_j (|f_1^i(\vec{x}) - f_1^j(\vec{x})| + |f_2^i(\vec{x}) - f_2^j(\vec{x})|)$  for all  $i, j = 1, 2, \dots, n$ ,  $a_i$  and  $b_i$  is the max and min value in the  $i^{th}$  objective. We get the approximated true Pareto fronts using all algorithm PF solutions combined in one solution to compute all metric results.

### B. RESULTS AND DISCUSSION

The performance metrics statistical results accomplished through the application of MOWSA, MOHTS, MOCBO, NSGWO, and MOMVO optimizers for eight truss test examples are elucidated in Tables 2-11.

#### 1) 10-BAR 2DTRUSS BENCHMARK

According to Table 2, the best  $f_{mean}$  result of HV metric is realized by proposed MOWSA among all that exhibit an 8.26% increase from MOMVO value at minimum  $f_{std}$ . MOWSA accomplished the highest FNRT value of 500, followed by MOHTS and MOCBO, thus representing its superior solution density in the propinquity of the Pareto Front. For GD indicator based on Table 3 MOWSA  $f_{mean}$  value illustrates a significant 61.10% and

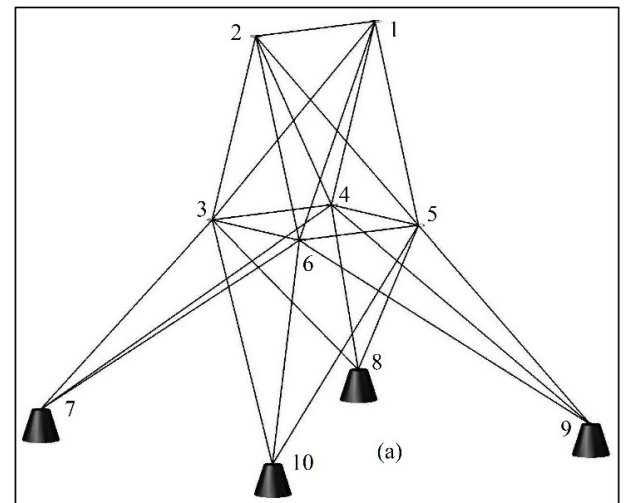


FIGURE 8. The 25-bar spatial truss.

36.83% decrease from MOMVO and MOHTS. Similarly, a 94.10%, 81.35%, 78.57%, and 66.01% decrease in  $f_{std}$  value are reported by MOWSA relative to MOMVO, MOHTS, MOCBO, and NSGWO, respectively. Moreover, MOWSA attains the best FNRT value of 125, which shows its enhanced convergence attribute regarding other optimizers. Regarding CVG performance measure as per Table 4, the MOMVO optimizer outperforms others; however, at a 95% significance value, MOWSA displays an enhanced coverage characteristic. Table 5 depicts the CPF metric  $f_{mean}$  result by the MOWSA has a significant percentage increase of 75.70% and 88.72% from MOMVO and NSGWO at superior  $f_{std}$  value. Moreover, MOWSA realizes the best FNRT value of 475, revealing its enhanced coverage over the Pareto Front feature. In terms of solution, diversity attribute driven by DM metric as stated in Table 6, the suggested MOWSA demonstrates its improved quality relatively as it achieves the best  $f_{mean}$ ,  $f_{std}$  results and settled at best FNRT values of 500 relatively. PD measure outcomes, according to Table 7, reveal that the MOWSA has a percentage increase of 54.03%, 14.37%, 10.64%, and 9.44% in  $f_{mean}$  value from



**TABLE 2. Results of (HV Metric) on truss bar problems.**

Algorithms	MOWSA	MOHTS	MOCBO	NSGWO	MOMVO	MOWSA	MOHTS	MOCBO	NSGWO	MOMVO
<b>10 bar</b>						<b>72 bar</b>				
$f_{min}$	0.6399425	0.63682004	0.63648817	0.62939223	0.58446699	0.66920143	0.68790155	0.66892966	0.68010376	0.61887934
$f_{max}$	0.64227248	0.63874373	0.63865521	0.63669962	0.60779829	0.69086857	0.69205951	0.68304769	0.68819742	0.64845608
$f_{mean}$	0.64111418	0.63765583	0.63784466	0.63252571	0.59219011	0.68425902	0.68975347	0.67476804	0.68564662	0.63207152
$f_{median}$	0.64112086	0.63752976	0.63811762	0.6320055	0.58824758	0.68848304	0.68952641	0.6735474	0.68714265	0.63047534
$f_{std}$	0.00108186	0.00081587	0.00097359	0.00312586	0.01097675	0.01012641	0.00198485	0.00610089	0.00373329	0.0132941
FNRT	500	350	350	200	100	400	475	200	325	100
<b>25 bar</b>						<b>120 bar</b>				
$f_{min}$	0.69502042	0.69428544	0.69060704	0.69173996	0.64769359	0.55237041	0.55244286	0.54756314	0.5490416	0.47972021
$f_{max}$	0.69575509	0.69517566	0.69189222	0.6938429	0.673532	0.55488	0.55415167	0.54998063	0.55022733	0.51664001
$f_{mean}$	0.69540008	0.6947503	0.69150433	0.69296146	0.66324135	0.55412256	0.553386614	0.54905443	0.54965104	0.49626905
$f_{median}$	0.6954124	0.69477004	0.69175904	0.69313148	0.6658699	0.5546199	0.55347501	0.54933697	0.54966762	0.49435799
$f_{std}$	0.00036513	0.00038916	0.00060177	0.00094896	0.01142066	0.00117938	0.0008176	0.00110617	0.00054746	0.01902469
FNRT	500	400	200	300	100	475	425	200	300	100
<b>37 bar</b>						<b>200 bar</b>				
$f_{min}$	0.6903485	0.69762574	0.69977843	0.69545129	0.62397123	0.74777623	0.72871705	0.76490123	0.75763856	0.68235765
$f_{max}$	0.70382605	0.70100658	0.70362961	0.70063695	0.63246218	0.76991707	0.76358039	0.78056528	0.7857116	0.733192
$f_{mean}$	0.69682695	0.6996071	0.70173602	0.69827206	0.62803795	0.75895504	0.75086943	0.77055099	0.77346736	0.71451834
$f_{median}$	0.69656662	0.69989804	0.70176802	0.69849999	0.6278592	0.75906344	0.75559014	0.76836872	0.77525965	0.72126185
$f_{std}$	0.00551566	0.00145075	0.00207876	0.0022324	0.0036253	0.01207844	0.01620452	0.00702604	0.013116	0.02240974
FNRT	275	350	475	300	100	325	250	425	400	100
<b>60 bar</b>						<b>942 bar</b>				
$f_{min}$	9938	0.53350635	0.41349182	0.51020045	0.44202174	0.6893325	0.68455839	0.71389486	0.7061757	0.68053346
$f_{max}$	0.53195877	0.54536367	0.50704563	0.53677684	0.4774159	0.72996827	0.7223464	0.72963682	0.73427013	0.69799145
$f_{mean}$	0.51563573	0.53859538	0.48209576	0.52750683	0.46686849	0.70382084	0.69679701	0.72003647	0.71777215	0.6902684
$f_{median}$	0.52034239	0.53775575	0.5039228	0.53152502	0.47401816	0.6979913	0.69014163	0.7183071	0.71532139	0.69127435
$f_{std}$	0.02029765	0.0057487	0.04576146	0.01238539	0.01676242	0.01836825	0.01731709	0.00744751	0.01190456	0.0086678
FNRT	300	475	200	400	125	325	225	425	375	150
Average FNRT	<b>3100</b>	<b>2950</b>	<b>2475</b>	<b>2600</b>	<b>875</b>	<b>1</b>	<b>2</b>	<b>4</b>	<b>3</b>	<b>5</b>

**TABLE 3. Results of (GD Metric) on truss bar problems.**

Algorithms	MOWSA	MOHTS	MOCBO	NSGWO	MOMVO	MOWSA	MOHTS	MOCBO	NSGWO	MOMVO
<b>10 bar</b>						<b>72 bar</b>				
$f_{min}$	13.5444011	19.7859075	15.8459095	14.3414343	24.1966512	14.7657797	27.8908376	44.8912285	26.14746	36.4770936
$f_{max}$	15.2627832	29.600088	25.0074654	19.4465671	56.862202	28.3801013	35.2063911	103.02387	71.5763292	55.7925718
$f_{mean}$	14.7646402	23.3759722	19.9583971	16.4420693	37.9615576	22.8093779	30.3181633	74.6728484	38.0318007	48.5526727
$f_{median}$	15.1256882	22.0589467	19.4901069	15.9901379	35.3936886	24.0458152	29.0877122	75.3881475	27.2017068	50.9705127
$f_{std}$	0.82040608	4.40006119	3.82848824	2.4139367	13.9258663	6.20211296	3.37322638	27.2852205	22.3721447	8.99898971
FNRT	125	400	300	175	500	125	275	450	250	400
<b>25 bar</b>						<b>120 bar</b>				
$f_{min}$	4.5482375	6.40106282	11.6074435	6.64661316	10.9462716	84.8094472	124.739491	138.794857	83.5611783	125.431305
$f_{max}$	6.17605666	8.158698812	16.1534775	7.41013133	15.4558112	101.187744	190.918482	174.468092	108.731124	215.577754
$f_{mean}$	5.3602045	7.45258182	13.1761294	7.0359425	13.3946874	92.0388785	148.310917	157.561643	93.5589364	179.004617
$f_{median}$	5.35826192	7.62528316	12.4717984	7.04351275	13.5883334	91.0791615	138.792848	158.491812	90.9717215	187.504704
$f_{std}$	0.66755358	0.77671261	2.11163597	0.34004341	1.87008552	6.98822552	31.0622932	16.187335	11.5404516	43.3337066
FNRT	100	275	450	225	450	175	375	375	125	450
<b>37 bar</b>						<b>200 bar</b>				
$f_{min}$	3.68112203	5.17268775	9.31844048	4.01192279	8.79561498	150.592588	102.970292	265.390731	186.542139	201.277648
$f_{max}$	4.37666257	6.22120353	13.3183662	8.87473562	17.5774197	324.967095	173.509001	443.75774	642.099021	269.794525
$f_{mean}$	4.11288325	5.62290405	11.2208661	6.02469946	12.7363189	241.708029	135.492414	361.169844	382.046579	224.584336
$f_{median}$	4.19687419	5.54886246	11.1233288	5.60606971	12.2861204	245.636216	132.745182	367.765452	349.772578	213.632585
$f_{std}$	0.30180256	0.48944138	1.95566918	2.04953729	4.10992884	84.0644062	37.0022245	80.0997355	211.704424	31.261016
FNRT	100	225	450	275	450	250	125	450	400	275
<b>60 bar</b>						<b>942 bar</b>				
$f_{min}$	10.1047111	13.875037	54.1828387	21.1420032	25.9807781	90123.0574	5572.67848	52425.7203	51587.6684	5434.19218
$f_{max}$	26.9121218	16.54405	106.332732	51.2805043	37.7637019	108434.751	14513.9631	96746.0828	76457.3421	10583.928
$f_{mean}$	16.3843519	15.569765	83.0415256	30.7386517	31.9767245	98617.3495	8105.46501	72450.6254	66278.5017	8057.4785
$f_{median}$	14.2602874	15.9299866	85.825266	25.2660497	32.081209	97955.7947	6167.60923	70315.3491	68534.4981	8105.89691
$f_{std}$	7.31064701	1.23142873	21.6395766	13.8865829	5.04780305	9537.89666	4293.86228	21688.8562	11642.9071	2150.20454
FNRT	175	150	500	300	375	500	125	350	350	175
Average FNRT	<b>1550</b>	<b>1950</b>	<b>3325</b>	<b>2100</b>	<b>3075</b>	<b>1</b>	<b>2</b>	<b>5</b>	<b>3</b>	<b>4</b>

MOMVO, MOCBO, NSGWO, and MOHTS, respectively. Also,  $f_{std}$  value of MOWSA reported a considerable percent reduction of 49.83%, 27.86%, and 26.92% from MOMVO, NSGWO, and MOCBO, respectively. MOWSA realizes the best FNRT value of 375 and exhibits its superior pure diversity behavior. Table 8 indicates the SP measure accordingly to the MOWSA  $f_{mean}$  the value reported a percentage decrease of 29.18%, 12.91%, 46.63%, and 84.63% from MOMVO, NSGWO, MOCBO, and MOHTS, respectively,

at minimum  $f_{std}$  results. The suggested MOWSA algorithm realizes the best FNRT value of 125 and outperforms others in spacing quality behavior at 95% significance value. Similarly, MOWSA outperforms others based on SD metric results reported in Table 9. There is a 67.86%, 69.52%, 54.76%, and 69.92% decrease reported by  $f_{mean}$  result of MOWSA concerning MOMVO, MOCBO, NSGWO, and MOHTS, respectively. MOWSA accomplished the best FNRT result of 125 and illustrated its non-dominated solutions fair

TABLE 4. Results of (CVG Metric) on truss bar problems.

Algorithms	MOWSA	MOHTS	MOCBO	NSGWO	MOMVO	MOWSA	MOHTS	MOCBO	NSGWO	MOMVO
	<b>10 bar</b>					<b>7 bar</b>				
$f_{min}$	0.82	0.61	0.80701754	0.68	0.53	0.78	0.9	0.98181818	0.89	0.75
$f_{max}$	0.88	0.96	0.90909091	0.81	0.61	0.82	0.99	1	0.99	0.93
$f_{mean}$	0.8525	0.78	0.86314041	0.75	0.57	0.8	0.94	0.99545455	0.9525	0.8475
$f_{median}$	0.855	0.775	0.8682266	0.755	0.57	0.8	0.935	1	0.965	0.855
$f_{std}$	0.02753785	0.14988885	0.04304518	0.05354126	0.04082483	0.02309401	0.0391578	0.00909091	0.04349329	0.08261356
FNRT	425	300	425	250	100	150	325	475	375	175
	<b>25 bar</b>					<b>120 bar</b>				
$f_{min}$	0.83	0.53	0.87692308	0.67	0.5	0.73	0.64	0.80392157	0.71	0.53
$f_{max}$	0.89	0.72	0.96825397	0.86	0.58	0.86	0.77	0.90384615	0.83	0.63
$f_{mean}$	0.86	0.6525	0.92737296	0.75	0.5375	0.775	0.71	0.84694193	0.75	0.6
$f_{median}$	0.86	0.68	0.93215739	0.735	0.535	0.755	0.715	0.84	0.73	0.62
$f_{std}$	0.0244949	0.08421203	0.04213611	0.08445906	0.035	0.05802298	0.05477226	0.04466625	0.05416026	0.04760952
FNRT	4387.5	187.5	500	300	125	387.5	250	450	312.5	100
	<b>37 bar</b>					<b>200 bar</b>				
$f_{min}$	0.87	0.88	0.93548387	0.96	0.87	0.53	1	1	1	1
$f_{max}$	0.96	0.97	1	0.99	0.97	0.81	1	1	1	1
$f_{mean}$	0.9	0.9175	0.97963368	0.9775	0.9275	0.6825	1	1	1	1
$f_{median}$	0.885	0.91	0.99152542	0.98	0.935	0.695	1	1	1	1
$f_{std}$	0.04082483	0.04112988	0.0304984	0.01258306	0.04645787	0.1158663	0	0	0	0
FNRT	187.5	212.5	450	412.5	237.5	100	350	350	350	350
	<b>60 bar</b>					<b>942 bar</b>				
$f_{min}$	0.62745098	0.94	1	1	0.96	0.1	0.81	1	1	1
$f_{max}$	0.73	1	1	1	1	0.31	1	1	1	1
$f_{mean}$	0.67436275	0.975	1	1	0.985	0.2425	0.945	1	1	1
$f_{median}$	0.67	0.98	1	1	0.99	0.28	0.985	1	1	1
$f_{std}$	0.04295069	0.02516611	0	0	0.01914854	0.09912114	0.09110434	0	0	0
FNRT	100	275	412.5	412.5	300	100	275	375	375	375
Average FNRT	1837.5	2175	3437.5	2787.5	1762.5	2	3	5	4	1

TABLE 5. Results of (CPF Metric) on truss bar problems.

Algorithms	MOWSA	MOHTS	MOCBO	NSGWO	MOMVO	MOWSA	MOHTS	MOCBO	NSGWO	MOMVO
	<b>10 bar</b>					<b>72 bar</b>				
$f_{min}$	0.75550197	0.72327606	0.68614951	0.39860546	0.39580033	0.58735663	0.60565919	0.61398152	0.4351955	0.22456176
$f_{max}$	0.80765496	0.75270071	0.7623896	0.42605982	0.49606449	0.73263866	0.6926206	0.68339168	0.51195796	0.30315763
$f_{mean}$	0.78114558	0.73470367	0.73332909	0.41391471	0.44456991	0.69427171	0.65135232	0.65680429	0.48363873	0.25553226
$f_{median}$	0.7807127	0.73141896	0.74238862	0.41549677	0.4432074	0.72854578	0.65356474	0.66492197	0.49370074	0.24720484
$f_{std}$	0.02299827	0.01261657	0.03637611	0.01245075	0.04116814	0.07132895	0.03573199	0.0316394	0.03560213	0.03586621
FNRT	475	350	375	125	175	450	375	375	200	100
	<b>25 bar</b>					<b>120 bar</b>				
$f_{min}$	0.81052664	0.7743394	0.67182929	0.46146743	0.44690619	0.71987732	0.72791088	0.66425303	0.35198604	0.34039157
$f_{max}$	0.82296761	0.81261985	0.78822517	0.55638212	0.54256521	0.76966495	0.74907035	0.71521876	0.4515241	0.47782812
$f_{mean}$	0.81662347	0.79048533	0.74208141	0.50604681	0.50475577	0.74697811	0.73838452	0.69755689	0.40572746	0.40846565
$f_{median}$	0.81649981	0.78749104	0.7541356	0.50316885	0.51477585	0.74918508	0.73827843	0.70537788	0.40969984	0.40782145
FNRT	500	400	300	150	150	475	425	300	150	150
	<b>37 bar</b>					<b>200 bar</b>				
$f_{min}$	0.67619092	0.6241675	0.69152292	0.43248728	0.26639355	0.5201457	0.28425355	0.61724135	0.20730243	0.08768831
$f_{max}$	0.74735076	0.70053777	0.83037954	0.54132085	0.3253846	0.64428085	0.40380972	0.7629828	0.37982305	0.24553464
$f_{mean}$	0.7103052	0.66697225	0.74305398	0.48334665	0.29969381	0.57063834	0.33805718	0.68773309	0.32513442	0.16118796
$f_{median}$	0.70883956	0.67159187	0.72515672	0.47978924	0.30349854	0.55906341	0.33208273	0.68535411	0.35670609	0.15576445
$f_{std}$	0.02933797	0.0337521	0.06172053	0.04476913	0.02753119	0.05712765	0.05010162	0.06645999	0.07955587	0.06545239
FNRT	450	325	425	200	100	400	225	500	275	100
	<b>60 bar</b>					<b>942 bar</b>				
$f_{min}$	0.39549549	0.46670597	0.35524915	0.34758946	0.1446578	0.17315457	0.06168032	0.22145834	0.12697243	0.03226011
$f_{max}$	0.61924139	0.59110258	0.60848901	0.53286896	0.34161212	0.30985738	0.15992083	0.49988978	0.21366535	0.05080136
$f_{mean}$	0.52358556	0.51293567	0.47979985	0.41500072	0.22695297	0.21528223	0.12132135	0.39395482	0.1572083	0.04230023
$f_{median}$	0.53980267	0.49696706	0.47773061	0.38977222	0.21077099	0.18905848	0.13184212	0.42723558	0.14409772	0.04306973
$f_{std}$	0.10587338	0.05782	0.10344666	0.08135305	0.08267709	0.06441516	0.04509956	0.12949456	0.04019635	0.00802309
FNRT	425	400	300	275	100	375	250	500	275	100
Average FNRT	3550	2750	3075	1650	975	1	3	2	4	5

distribution. Referring to the IGD as specified in Table 10, MOWSA realizes the best  $f_{mean}$  value, i.e., 1043.04136, followed by MOHTS. As per the FNRT test, MOWSA realized the second-best value of 175 after MOHTS settled at 150 values. Thus, at a 95% significance value, MOWSA displays its enhanced convergence-spread equivalence against all. Table 11 depicts the RT metric results according to which MOWSA found the best  $f_{mean}$ ,  $f_{std}$  values, i.e., 12.7284798, 1.9189647 amongst contrasted algorithms. Its

best FNRT value, i.e., 125, shows its minimum computational cost to achieve the optimal solution against other optimizers. Table 12 reveals the BCS that satisfied each objective ( $f_{weight}$ ,  $f_{compliance}$ ) depending on the fuzzy decision method. As can be seen from the table, MOWSA has outstanding BCS results, i.e., (3323.2601, 153080.53) of any of the algorithms tested.

The qualitative behavior of all considered algorithms is illustrated through their corresponding best Pareto fronts and

**TABLE 6. Results of (DM Metric) on truss bar problems.**

Algorithms	MOWSA	MOHTS	MOCBO	NSGWO	MOMVO	MOWSA	MOHTS	MOCBO	NSGWO	MOMVO
<b>10 bar</b>						<b>72 bar</b>				
$f_{min}$	0.80418182	0.4778	0.7525	0.6393	0.6388	0.81272727	0.4561	0.7135	0.6449	0.3643
$f_{max}$	0.87947368	0.5769	0.8047	0.7149	0.6965	0.87844828	0.5686	0.7857	0.7083	0.4536
$f_{mean}$	0.84052441	0.52795	0.78145	0.681975	0.6668	0.84056661	0.493775	0.760425	0.6747	0.4031
$f_{median}$	0.83922106	0.52855	0.7843	0.68685	0.66595	0.83554545	0.4752	0.77125	0.6728	0.39725
$f_{std}$	0.03171715	0.04248251	0.0239624	0.03151395	0.02670069	0.02755887	0.0517067	0.03311288	0.02753846	0.0380462
FNRT	500	100	400	275	225	500	200	400	300	100
<b>25 bar</b>						<b>120 bar</b>				
$f_{min}$	0.83424242	0.5519	0.7085	0.633	0.6572	0.803	0.5928	0.7501	0.6088	0.5772
$f_{max}$	0.86333333	0.6003	0.7839	0.716	0.7213	0.90923077	0.6285	0.7792	0.664	0.6947
$f_{mean}$	0.84247603	0.5753	0.752875	0.689975	0.689875	0.85247436	0.606125	0.759475	0.640625	0.65675
$f_{median}$	0.83616418	0.5745	0.75955	0.70545	0.6905	0.84883333	0.6016	0.7543	0.64485	0.67755
$f_{std}$	0.01401474	0.02694043	0.03212708	0.03838319	0.02863126	0.04594044	0.0158941	0.01344182	0.02306547	0.0543332
FNRT	500	100	400	250	250	500	125	400	225	250
<b>37 bar</b>						<b>200 bar</b>				
$f_{min}$	0.77634921	0.5454	0.7425	0.6649	0.4652	0.69583333	0.4334	0.6624	0.4863	0.2634
$f_{max}$	0.8383871	0.5786	0.7665	0.7258	0.5168	0.79308642	0.5252	0.7267	0.5631	0.3827
$f_{mean}$	0.81838747	0.56285	0.754525	0.695975	0.5027	0.72479305	0.4618	0.7049	0.53475	0.31095
$f_{median}$	0.82940678	0.5637	0.75455	0.6966	0.5144	0.70512622	0.4443	0.71525	0.5448	0.29885
$f_{std}$	0.02838808	0.01366004	0.0138276	0.02501831	0.02506405	0.04585111	0.04258419	0.02884429	0.0349316	0.05476401
FNRT	500	200	400	300	100	450	225	450	275	100
<b>60 bar</b>						<b>942 bar</b>				
$f_{min}$	0.58933333	0.4836	0.63527473	0.6604	0.3236	0.51682692	0.31709866	0.38350647	0.39214047	0.11852007
$f_{max}$	0.78216216	0.5177	0.7079	0.7324	0.43490196	0.71474045	0.37980769	0.60566472	0.50898829	0.1812291
$f_{mean}$	0.67363145	0.49985	0.67734368	0.693375	0.38665049	0.63736018	0.33823683	0.48522131	0.44996342	0.16293896
$f_{median}$	0.66151515	0.49905	0.6831	0.69035	0.39405	0.65893667	0.32802048	0.47585702	0.44936246	0.17600334
$f_{std}$	0.08581841	0.01405193	0.03114951	0.03002359	0.0493549	0.08457216	0.02819071	0.09147203	0.05128466	0.03001966
FNRT	375	200	400	425	100	500	200	350	350	100
Average FNRT	<b>3825</b>	<b>1350</b>	<b>3200</b>	<b>2400</b>	<b>1225</b>	<b>1</b>	<b>4</b>	<b>2</b>	<b>3</b>	<b>5</b>

**TABLE 7. Results of (PD Metric) on truss bar problems.**

Algorithms	MOWSA	MOHTS	MOCBO	NSGWO	MOMVO	MOWSA	MOHTS	MOCBO	NSGWO	MOMVO
<b>10 bar</b>						<b>72 bar</b>				
$f_{min}$	57966910.95	52114663.52	51838044.66	53783885.25	33395812.04	59817741.78	43023633.15	41150701.4	60017132.35	32836791.87
$f_{max}$	73836922.12	69946862.57	73416695.05	76290111.18	64743296.52	69519306.6	65808682.02	57137539.51	62163809.05	43089703.28
$f_{mean}$	68275850.82	62384875.85	59693297.69	61705677.16	44324229.1	66449641.33	54456274.98	47584370.87	60790879.94	35969952.66
$f_{median}$	70649785.1	63738988.66	56759225.53	58374356.1	39578903.92	68230758.48	54496392.38	46024621.29	60491289.17	33976657.74
$f_{std}$	7189196.335	7446036.714	9837789.207	9966182.218	14330045.36	4468747.331	9549896.23	6818974.253	948039.9099	4845722.516
FNRT	375	325	300	300	200	450	325	225	400	100
<b>25 bar</b>						<b>120 bar</b>				
$f_{min}$	29125755.79	23426867.83	26369408.9	26127796.99	16992820.7	438660979.5	350887222.2	337838453.2	404726883.9	224063253.7
$f_{max}$	45920732.65	30394474.02	32207641.14	39436743.97	33174662.87	662203419	464689113.2	415855007.3	529724628.1	413426997.9
$f_{mean}$	38154189.09	27224403.3	28928972.32	33600235.53	27682605.42	535205438.4	407336107.2	388062947.6	472878201	318390476.6
$f_{median}$	38785133.96	27538135.67	28569419.61	34418200.58	30281469.05	519978677.5	406884046.7	399279165	478530645.9	318035827.5
$f_{std}$	8091908.22	3026102.715	2703664.257	5649933.857	7363229.037	106407690.7	46522145.39	34726974.32	57036054.73	79489463.42
FNRT	450	200	250	350	250	475	275	200	375	175
<b>37 bar</b>						<b>200 bar</b>				
$f_{min}$	13003561.37	10768527.74	16036840.42	13676892.64	6235376.358	108192145.1	49333508.15	114004402.3	111169810.4	45336402.71
$f_{max}$	18476017.52	12590194.72	17351165.8	15044754.16	8887748.995	256961677.1	121255724.2	156643540.4	161265528.9	77149363.49
$f_{mean}$	14975200.24	11662029.33	16434487.86	14121553.02	7665673.606	156734946.4	76329408.93	130466930.8	130388925.7	62789959.95
$f_{median}$	14210611.03	11644697.42	16174972.61	13882282.65	7769784.535	130892981.7	67364201.68	125609890.2	124560181.8	64337036.8
$f_{std}$	2424963.52	911951.9541	622456.746	628667.0889	1094803.433	67820034.52	31321048.46	18853424.91	21569424.31	13416812.6
FNRT	400	200	475	325	100	425	225	375	350	125
<b>60 bar</b>						<b>942 bar</b>				
$f_{min}$	15667966.95	16765109.24	8360066.626	20111085.94	9001407.776	6100604033	3484482498	8311654850	7235590126	1380313029
$f_{max}$	22339929	24490974.99	20077247.81	26259677.06	16228164.71	11496377298	4371910630	12553474530	12697839337	2216950513
$f_{mean}$	20288087.73	21382877.82	15833540.12	22811644.77	12372147.38	8808994882	3881726317	9806817218	9322750670	1873978702
$f_{median}$	21572227.49	22137713.52	17448423.03	22437908.03	12129508.51	8819499100	3835256070	9181069745	8678786608	1949325633
$f_{std}$	3109267.994	3666523.379	5269791.392	2866227.55	3130680.732	2203184616	424005980.3	1963168644	2351036691	366072025.7
FNRT	350	400	175	425	150	375	200	425	400	100
Average FNRT	<b>3300</b>	<b>2150</b>	<b>2425</b>	<b>2925</b>	<b>1200</b>	<b>1</b>	<b>4</b>	<b>3</b>	<b>2</b>	<b>5</b>

combined behavior, as shown in Figure 6. As per comparative analysis, MOWSA provides smooth, continuous, and diverse solutions. Box plots were constructed to demonstrate the quantitative behavior of considered algorithms in terms of the performance measure (as shown in Figure 7), which depict the superior behavior of MOWSA concerning other optimizers.

2) 25-BAR 3D TRUSS BENCHMARK

Figure 8 shows a 25-bar spatial truss. The first performance measure (i.e., HV) results are depicted in Table 2, according

to which the proposed MOWSA optimizer realizes the best  $f_{mean}$  value of 0.69540008, followed by MOHTS. The FNRT results accomplished by MOWSA, MOHTS, MOCBO, NSGWO, and MOMVO are 500,400, 200, 300, and 100, respectively. At a 95% significance value, MOWSA demonstrates its superior solutions density near the Pareto Front relative to other algorithms. GD metric is the second efficiency measure that computational results are illustrated in Table 3 accordingly MOWSA  $f_{mean}$  value presents a percentage decrease of 59.98%,23.81%,59.31%, and 28.07% from MOMVO, NSGWO, MOCBO, and MOHTS,



TABLE 8. Results of (SP Metric) on truss bar problems.

Algorithms	MOWSA	MOHTS	MOCBO	NSGWO	MOMVO	MOWSA	MOHTS	MOCBO	NSGWO	MOMVO
	10bar					72 bar				
$f_{min}$	331.766618	2721.58702	757.777066	472.116861	461.770358	214.554899	927.157406	428.214904	403.549431	148.650498
$f_{max}$	685.400142	3932.88996	1030.1414	584.67976	760.301823	609.46907	1424.32682	1188.56948	479.323445	583.713844
$f_{mean}$	468.141681	3046.62474	877.282105	537.58322	661.031878	417.175849	1201.17921	857.972307	439.745978	315.863075
$f_{median}$	427.699982	2766.01099	860.604978	546.76813	711.027666	422.339712	1226.6163	907.552424	438.051017	265.54398
$f_{std}$	155.390079	591.924626	115.102177	53.1181625	137.866259	165.16495	209.631268	333.895598	41.2849327	196.36688
FNRT	125	500	400	200	275	225	500	350	250	175
	25 bar					120 bar				
$f_{min}$	04.296281	762.020682	279.713895	253.435787	133.541108	2136.82565	13425.2055	5784.15041	4567.42846	3788.94609
$f_{max}$	123.439369	1177.12397	303.365071	317.178985	523.2147	2474.57037	21146.6619	8064.34421	5983.91243	15990.1555
$f_{mean}$	14.696756	1005.74883	295.234705	285.4137	327.881754	2338.32308	17335.7245	6566.66393	5229.70266	8825.03175
$f_{median}$	115.525687	1041.92533	298.929927	285.520013	327.385603	2370.94814	17385.5153	6209.08054	5183.73488	7760.51268
$f_{std}$	17780196	202.457242	10.6616231	26.2379769	159.562149	145.385995	3154.43404	1045.12394	635.665912	5375.18668
FNRT	100	500	300	275	325	100	500	325	250	325
	37 bar					200 bar				
$f_{min}$	44.207065	275.143004	101.994939	107.887472	46.7224932	233.161102	1583.0855	686.25327	666.187506	244.103185
$f_{max}$	128.871115	446.234293	160.680835	244.584401	70.1516035	397.86582	2480.50806	1520.60546	1352.62643	417.082046
$f_{mean}$	3.0413171	372.171633	123.331318	154.938158	55.2921594	299.997598	1882.18793	990.645248	1109.19661	310.545665
$f_{median}$	79.5435444	383.654618	115.324748	133.640379	52.1472704	284.481735	1732.57908	877.861134	1208.98625	290.498714
$f_{std}$	40.7288263	83.0539622	25.8576528	62.0882876	11.0005605	74.0671174	409.676916	383.741807	305.004769	78.0404428
FNRT	200	500	300	350	150	150	500	350	350	150
	60 bar					942 bar				
$f_{min}$	106.441856	370.934279	198.770922	141.959432	141.913765	25256.3332	79398.9812	59907.045	75795.95	18996.3104
$f_{max}$	325.133045	4210.00662	641.431047	601.447066	799.350084	43370.4495	146823.948	89822.8491	120490.333	36117.8332
$f_{mean}$	179.040443	1470.4518	431.832333	292.35623	448.215148	34005.9137	107620.474	76336.4296	99592.0671	28366.3696
$f_{median}$	142.293436	650.433149	443.563682	213.009212	425.798372	33698.4361	102129.483	77807.9121	101040.993	29175.6674
$f_{std}$	99.8370642	1831.6013	181.238864	213.952209	338.713407	8568.44138	28309.4683	13798.7343	23497.3059	8902.31304
FNRT	175	475	350	225	275	150	475	300	425	150
Average FNRT	1225	3950	2675	2325	1825	1	5	4	3	2

TABLE 9. Results of (SD Metric) on truss bar problems.

Algorithms	MOWSA	MOHTS	MOCBO	NSGWO	MOMVO	MOWSA	MOHTS	MOCBO	NSGWO	MOMVO
	10 bar					72 bar				
$f_{min}$	0.23990554	0.9569643	0.61346385	0.95788849	0.88621934	0.46497414	0.81018414	0.57247779	0.8555047	0.88462008
$f_{max}$	0.34441773	1.0585666	0.76538632	1.01422202	0.95925064	0.57747171	0.87865162	0.78160601	0.884771	0.96160264
$f_{mean}$	0.29852172	0.99273231	0.65996655	0.97957429	0.92905909	0.53743594	0.84835317	0.69570599	0.86706252	0.90782728
$f_{median}$	0.30488181	0.97769917	0.63050802	0.97309332	0.9353832	0.55364895	0.85228847	0.71437007	0.86398718	0.8925432
$f_{std}$	0.04416464	0.04511459	0.07074165	0.02423082	0.03103517	0.05065492	0.02856908	0.08816199	0.01301285	0.0360798
FNRT	100	450	200	450	300	100	350	200	350	500
	25 bar					120 bar				
$f_{min}$	0.17700114	0.84584237	0.56507456	0.81080809	0.83414692	0.18143812	0.86066455	0.59531385	0.94733711	0.93887017
$f_{max}$	0.23129129	0.97884098	0.57563243	0.88437043	0.8939542	0.22996621	0.97321703	0.75336452	1.0206138	1.0826606
$f_{mean}$	0.20366592	0.91858	0.57016302	0.85490294	0.86539347	0.20310314	0.91106589	0.670348	0.97755411	0.98230592
$f_{median}$	0.20318562	0.92481831	0.56997254	0.86221663	0.86673639	0.20050412	0.90519099	0.6663568	0.97113276	0.95384646
$f_{std}$	0.02374006	0.06348991	0.00523989	0.03178806	0.02737978	0.02016507	0.04694141	0.06469494	0.0319281	0.06745214
FNRT	100	450	200	350	400	100	300	200	450	450
	37 bar					200 bar				
$f_{min}$	0.45095755	0.73665801	0.60041635	0.81919748	0.86562681	0.78548375	0.63210976	0.59447281	0.90416945	0.90995614
$f_{max}$	0.55107424	0.93877519	0.74917652	0.90907983	0.92131378	0.84581074	0.77405579	0.759342	0.96503318	0.95598981
$f_{mean}$	0.50795124	0.86124658	0.67783758	0.86388522	0.89936086	0.81433292	0.69585352	0.68545435	0.94073525	0.92856795
$f_{median}$	0.51488658	0.88477656	0.68087872	0.86363179	0.90525143	0.8130186	0.68862426	0.69400129	0.94686919	0.92416294
$f_{std}$	0.04661644	0.09594163	0.07299969	0.04194229	0.02404967	0.02591723	0.06505704	0.06943587	0.02865748	0.01987609
FNRT	100	400	225	350	425	300	150	150	475	425
	60 bar					942 bar				
$f_{min}$	0.4763186	0.90375571	0.86309013	0.92797735	0.9808209	0.84806841	0.65830374	0.83432673	0.88206236	0.96144181
$f_{max}$	0.63268815	1.21466222	0.93810177	0.97201074	1.10041325	0.87376687	0.79788498	0.89543994	1.00493636	0.98110557
$f_{mean}$	0.56910177	1.00903334	0.90774583	0.94287854	1.03090715	0.86316359	0.70992131	0.86715326	0.94695432	0.97258233
$f_{median}$	0.58370016	0.95885772	0.91489571	0.93576303	1.02119722	0.86540954	0.69174826	0.86942319	0.95040928	0.97389098
$f_{std}$	0.07599121	0.14022233	0.03246792	0.02028875	0.05173687	0.01245472	0.06612637	0.02959018	0.05759273	0.00929264
FNRT	100	400	225	300	475	250	100	275	425	450
Average FNRT	1150	2600	1675	3150	3425	1	3	2	4	5

respectively. MOWSA realizes the best FNRT value of 100, revealing its convergence behavior excellence amongst other algorithms. As per Table 4, the best CVG metric  $f_{mean}$  the result is reported by the MOMVO algorithm, while the least  $f_{std}$  value is realized by MOWSA. MOWSA displays its enhanced coverage characteristic. Table 5 presents the CPF metric outcomes that illustrate the MOWSA realizes the best  $f_{mean}$  the value that exhibits a significant increase of 61.78% and 61.37% from MOMVO and NSGWO, respectively.

Moreover, in terms of  $f_{std}$ , the MOWSA algorithm value reported a significant decrease of 87.36%, 89.22%, 90.45%, and 70.18% relative to MOMVO, NSGWO, MOCBO, and MOHTS, respectively. MOWSA found the best FNRT value of 500, followed by MOHTS, which manifests its enhanced coverage over the Pareto Front feature. DM metric computational analysis, as stated in Table 6, shows that the best  $f_{mean}$  value is 0.84247603 is realized by MOWSA relatively at least 0.01401474  $f_{std}$  value. The



**TABLE 10. Results of (IGD Metric) on truss bar problems.**

Algorithms	MOWSA	MOHTS	MOCBO	NSGWO	MOMVO	MOWSA	MOHTS	MOCBO	NSGWO	MOMVO
<b>10 bar</b>						<b>72 bar</b>				
$f_{min}$	587.586348	753.469594	1382.19937	2484.54449	7596.45202	735.932401	1962.38732	3010.02654	1183.86859	7305.26553
$f_{max}$	1466.45708	1391.22706	2219.41146	5831.31744	17805.9446	2334.37293	3046.50004	4988.16854	2142.12165	10546.1941
$f_{mean}$	1043.04136	1109.38202	1747.85864	4060.01335	13508.7516	1226.13441	2442.63967	3785.35683	1743.65696	9357.82433
$f_{median}$	1059.06101	1146.41571	1694.91186	3962.09572	14316.3049	917.116164	2380.83566	3571.61612	1824.31879	9789.91885
$f_{std}$	479.924228	286.289199	348.19138	1650.04312	4776.4521	743.984921	485.884839	850.175737	402.219475	1428.61454
FNRT	175	150	275	400	500	150	275	400	175	500
<b>25 bar</b>						<b>120 bar</b>				
$f_{min}$	174.242704	186.790327	376.754977	271.477377	2488.65365	5204.59553	4139.37435	11993.7559	10269.3149	70203.2802
$f_{max}$	202.774937	271.987935	491.038498	614.395312	4594.40357	12393.8137	5581.66626	20977.0197	22215.6653	153877.184
$f_{mean}$	187.977599	234.860756	455.663467	478.674028	3677.42266	7107.83968	4762.04929	15571.5141	15575.4382	107801.392
$f_{median}$	187.446379	240.332381	477.430197	514.411712	3813.31671	5416.47475	4663.57826	14657.6404	14908.3862	103562.552
$f_{std}$	11.6860415	38.7374584	53.2355389	157.391369	889.322873	3525.79409	633.362436	4274.10779	4978.27867	40305.0917
FNRT	100	200	350	350	500	175	125	350	350	500
<b>37 bar</b>						<b>200 bar</b>				
$f_{min}$	174.41122	387.679908	209.364703	259.255413	2457.72917	8151.82621	22028.1733	4506.67583	3621.64509	29876.5477
$f_{max}$	441.098347	510.188367	289.329658	481.890992	3609.96362	11799.3955	33331.0498	6386.47112	15838.6515	43353.6875
$f_{mean}$	329.868686	451.634502	242.749354	369.693975	3269.37337	9366.07518	27345.7585	5573.30791	7674.25279	36662.026
$f_{median}$	351.982587	454.334867	236.151528	368.814748	3504.90034	8756.5395	27011.9054	5700.04234	5618.35729	36708.9343
$f_{std}$	126.320685	51.2088614	34.8413396	112.193742	546.158263	1689.31418	5175.05449	781.363667	5758.18307	5503.48282
FNRT	200	375	150	275	500	275	425	150	175	475
<b>60 bar</b>						<b>942 bar</b>				
$f_{min}$	586.565771	1181.39413	3013.88437	1337.05084	4177.09005	1839613.9	4115679.22	1208912.36	1635279.73	6004193.73
$f_{max}$	3177.08063	2094.47328	9267.6905	2563.22968	5132.37592	3747405.42	4519660.49	2314745.85	2723935.94	6756452.89
$f_{mean}$	1950.89227	1565.73856	4730.19191	1987.47121	4552.95763	2943662.88	4395037.38	1741833.87	2188913.02	6250168.24
$f_{median}$	2019.96135	1493.5434	3319.59638	2024.80216	4451.18228	3093816.09	4472404.91	1721838.64	2198218.21	6120013.18
$f_{std}$	1307.81456	451.130239	3028.53702	569.858108	408.187746	798162.831	188256.205	452456.545	512254.832	344798.776
FNRT	200	175	425	225	475	275	400	150	175	500
Average FNRT	<b>1550</b>	<b>2125</b>	<b>2250</b>	<b>2125</b>	<b>3950</b>	<b>1</b>	<b>2</b>	<b>3</b>	<b>2</b>	<b>4</b>

**TABLE 11. Results of (RUNTIME - RT Metric) on truss bar problems.**

Algorithms	MOWSA	MOHTS	MOCBO	NSGWO	MOMVO	MOWSA	MOHTS	MOCBO	NSGWO	MOMVO
<b>10 bar</b>						<b>72 bar</b>				
$f_{min}$	10.5213411	14.1487302	10.6960773	14.14784	24.913219	72.1905577	75.0343495	72.4040684	78.2558289	89.3795855
$f_{max}$	14.36373	18.5264085	14.7264868	18.657076	35.9445211	100.143104	103.896628	100.540081	105.241281	121.793864
$f_{mean}$	12.7284798	16.3301131	13.1796343	16.4969339	30.3285841	89.4250435	91.7338603	87.9101423	94.2965763	108.618912
$f_{median}$	13.0144241	16.3226569	13.6479866	16.5914099	30.2282981	92.6832563	94.002232	89.3482101	96.8445975	111.651099
$f_{std}$	1.9189647	2.39071097	1.92960075	2.49325576	6.11577888	13.3023401	14.4213962	14.5589738	13.1941693	15.9277881
FNRT	125	325	175	375	500	150	275	175	400	500
<b>25 bar</b>						<b>120 bar</b>				
$f_{min}$	27.1502526	31.3069429	27.3953077	31.6711413	43.8056279	127.152875	130.632417	127.466108	135.719939	147.106121
$f_{max}$	37.2144893	42.7929091	37.6328076	42.0064658	59.35494	170.452041	174.796067	171.364298	176.901978	197.099897
$f_{mean}$	32.2667082	39.2224805	32.6020993	37.5779524	51.8396167	152.793184	157.120796	152.627428	157.692005	175.744521
$f_{median}$	32.3510454	41.395035	32.6901409	38.3171012	52.0989494	156.78391	161.527349	155.839652	159.073051	179.386033
$f_{std}$	5.70766626	5.37405716	5.72529226	5.15516592	8.63560714	21.3920128	21.6376747	22.2519126	22.2886924	25.0002703
FNRT	100	375	200	325	500	150	325	175	350	500
<b>37 bar</b>						<b>200 bar</b>				
$f_{min}$	35.6958443	38.738372	36.0060555	40.0181229	51.4587055	196.365252	199.842701	197.847676	204.140988	214.094088
$f_{max}$	48.8296987	52.8406426	49.4686791	53.5889835	70.949893	261.399889	264.849886	262.5723	267.973388	284.606694
$f_{mean}$	42.4192311	47.5276922	42.8810996	46.8152681	62.998902	231.093306	232.242777	235.529842	236.13888	250.606407
$f_{median}$	42.5756907	49.2658771	43.0248318	46.826983	64.7935048	233.30404	232.13926	240.849695	236.220571	251.862422
$f_{std}$	7.40508467	6.73368966	7.52168612	7.718173	9.24384587	35.1492526	37.3741404	32.1368287	36.7457909	38.7241889
FNRT	100	325	200	375	500	150	250	250	350	500
<b>60 bar</b>						<b>942 bar</b>				
$f_{min}$	63.7453297	66.161201	64.2644823	69.3262373	80.3214033	1001.1338	1002.33582	1005.01575	1011.92636	1018.45026
$f_{max}$	90.4220252	93.8313086	89.5632774	94.0092934	110.89257	1327.81898	1328.41879	1332.32011	1342.71733	1349.00281
$f_{mean}$	78.3537122	80.3734629	78.3930249	82.854131	95.8219964	1166.44447	1171.55735	1173.70753	1175.75985	1184.91796
$f_{median}$	79.623747	80.750671	79.8721699	84.0404966	96.0370062	1168.41256	1177.7374	1178.74712	1174.19785	1186.10937
$f_{std}$	13.2780825	14.6004934	12.9612549	12.9759071	16.9082543	183.637506	180.891029	180.720552	186.815126	188.696413
FNRT	150	250	200	400	500	125	275	325	325	450
Average FNRT	<b>1050</b>	<b>2400</b>	<b>1700</b>	<b>2900</b>	<b>3950</b>	<b>1</b>	<b>3</b>	<b>2</b>	<b>4</b>	<b>5</b>

FNRT values gained by MOWSA, MOCBO, NSGWO, MOMVO, and MOHTS are 500, 400, 250, 250 and 100, respectively. At 95% significance value, MOWSA exhibits enhanced solution diversity. The PD results are illustrated in Table 7, whereby MOWSA  $f_{mean}$  value shows a percentage increase of 37.82%, 13.55%, 31.88%, and 40.14% from MOMVO, NSGWO, MOCBO, and MOHTS, respectively. The FNRT value accomplished by MOWSA, MOHTS, MOCBO, NSGWO, and MOMVO is 450, 200, 250,350, and

250, respectively. At a 95% significance value, MOWSA outperforms other compared algorithms in terms of solution pure diversity attributes. Table 8 governs the SP metric results that demonstrate  $f_{mean}$  value of the MOWSA has a percentage decrease of 65.01%, 59.81%, 61.15%, and 88.59% from MOMVO, NSGWO, MOCBO, and MOHTS, respectively. Moreover,  $f_{std}$  value of MOWSA reported a 94.24%, 65.02%, 13.91%, and 95.46% decrease from MOMVO, NSGWO, MOCBO, and MOHTS algorithms,

TABLE 12. The Best Compromise Solution (BCS) results of all algorithms.

Algorithms	MOWSA	MOHTS	MOCBO	NSGWO	MOMVO
<b>10 - bar truss (Best Compromise Solution)</b>					
$f_{weight}$	3323.2601	5989.9493	7561.5833	7979.8648	9398.4436
$f_{compliance}$	153080.53	82332.867	64697.565	61127.988	51984.992
<b>25 - bar truss (Best Compromise Solution)</b>					
$f_{weight}$	2362.3432	4047.7732	4391.3361	4400.5384	5147.418
$f_{compliance}$	34997.369	19803.421	18201.681	18153.119	15739.877
<b>37 - bar truss (Best Compromise Solution)</b>					
$f_{weight}$	1244.4363	1887.1162	2652.3757	2269.0725	2477.5399
$f_{compliance}$	17721.946	11393.115	8072.9159	9428.7458	8965.0961
<b>60 - bar truss (Best Compromise Solution)</b>					
$f_{weight}$	1852.5902	4062.5842	5536.4407	5570.8908	5459.924
$f_{compliance}$	78036.883	33706.85	25066.981	24401.347	25773.127
<b>72 - bar truss (Best Compromise Solution)</b>					
$f_{weight}$	6046.4369	8552.75	12218.189	12133.744	14432.509
$f_{compliance}$	72102.582	47540.165	32899.733	33121.221	28324.217
<b>120 - bar truss (Best Compromise Solution)</b>					
$f_{weight}$	19060.176	44365.829	47505.369	48082.821	58210.282
$f_{compliance}$	1546234.8	662789.68	619171.47	611591.35	509698.23
<b>200 - bar truss (Best Compromise Solution)</b>					
$f_{weight}$	23201.131	42239.563	42263.722	31321.168	39418.704
$f_{compliance}$	74750.126	36793.587	45709.931	48928.751	38243.298
<b>942 - bar truss (Best Compromise Solution)</b>					
$f_{weight}$	5857383.8	10085976	8617931.3	7978704.6	6764594.8
$f_{compliance}$	2802136.4	1272896.9	1556975.3	1662949	1551334.7

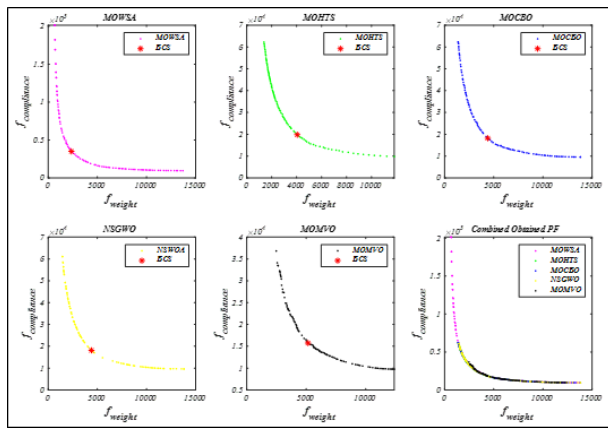


FIGURE 9. Best Pareto fronts of considered algorithms for 25-bar truss.

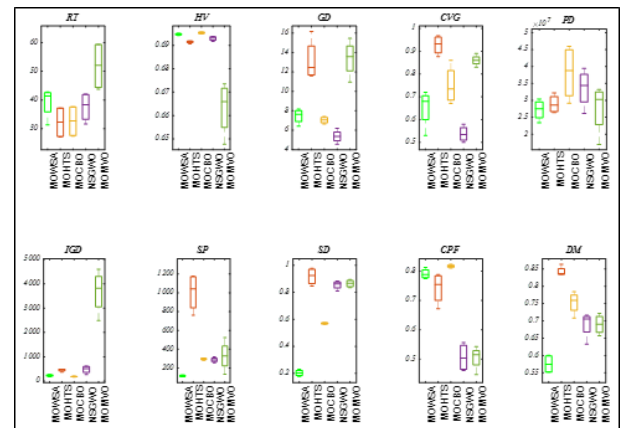


FIGURE 10. Box plots of considered algorithms for 25-bar truss.

respectively. The MOWSA realizes the best FNRT value of 100, which relatively presents its best spacing feature. SD performance measure outcomes, as depicted in Table 9, indicate that the best  $f_{mean}$  value, i.e., 0.20366592, is attained by MOWSA, is 64.27%, 76.17%, 76.46%, and 77.82% less than MOCBO, NSGWO, MOMVO, and MOHTS, respectively. The FNRT results of MOWSA, MOHTS, MOCBO, NSGWO, and MOMVO are 100,450,200,350,400, respectively. These findings manifest the well-distribution of MOWSA NDS relative to others. As per the IGD metric computational analysis that is illustrated in Table 10, the  $f_{mean}$  value of MOWSA exhibits a substantial percentage decrease of 94.88%, 60.72%, 58.74%, and 19.96% from MOMVO, NSGWO, MOCBO, and MOHTS, respectively. Additionally, MOWSA realize a 98.68%, 92.57%, 78.04%, 69.83% decrease of  $f_{std}$  value against MOMVO, NSGWO, MOCBO,

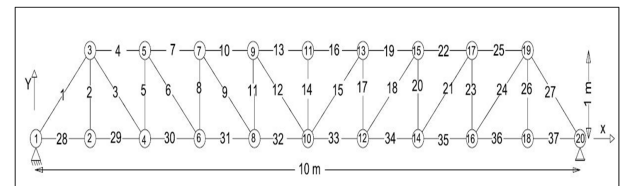


FIGURE 11. The 37-bar truss.

and MOHTS optimization methodologies, respectively. Following FNRT inspection, the proposed MOWSA uncovers the best result of 100, and at 95% significance value, it relatively reveals its superior property of convergence-spread equivalence. Table 11 indicates the RT metric results as per the best  $f_{mean}$  value of 32.2667082 reported by MOWSA, which is less than other contrasted optimization techniques. The FNRT results of MOWSA, MOHTS,

MOCBO, NSGWO, and MOMVO are 100, 375, 200, 325, and 500, respectively. At a 95% significance value, MOWSA portrays its dominance in terms of the least computational time to find the optimal solutions relatively. According to Table 12, the proposed MOWSA realizes the  $f_{weight}$  value of 2362.3432 and the 34997.369 value for  $f_{compliance}$  that is the best BCS among all.

Figure 9 illustrates the qualitative behavior of all five algorithms in terms of their best Pareto fronts and corresponding BCS results. Moreover, the figure presents the comparative analysis through combined Pareto fronts according to which the MOWSA solutions are well spread, continuous, and smooth. The quantitative superiority of the proposed MOWSA technique over the others is depicted in Figure 10 for all examined performance metric implications.

### 3) 37-BAR 2D TRUSS BENCHMARK

Figure 11 shows a 37-bar truss structure. According to Table 2, the best  $f_{mean}$  result of the HV metric is realized by MOCBO among all, while the least  $f_{std}$  result is reported by MOHTS. According to FNRT analysis, the highest rank is achieved by MOCBO, which governs its refined solutions density near the Pareto Front. For GD indicator based on Table 3 MOWSA  $f_{mean}$  value illustrates a significant 67.70% and 63.34% decrease from MOMVO and MOCBO. Similarly, a 92.65%, 85.27%, 84.56%, and 38.33% decrease in  $f_{std}$  value is reported by MOWSA relative to MOMVO, NSGWO, MOCBO, and MOHTS, respectively. Moreover, MOWSA attains the best FNRT value of 100, which shows its enhanced convergence attribute regarding other optimizers. In terms of CVG performance measures as per Table 4, the MOWSA optimizer outperforms others by realizing the best  $f_{mean}$  and FNRT results of 0.9 and 187.5, respectively. Also, at a 95% significance value, MOWSA displays enhanced coverage characteristics among other algorithms. Table 5 depicts that the MOWSA CPF metric  $f_{mean}$  result has a significant percentage increase of 137.01% and 46.95% from MOMVO and NSGWO at superior  $f_{std}$  value. Moreover, MOWSA realizes the best FNRT value of 450, revealing its improved coverage rate over the Pareto Front attribute. Table 6 presents the DM metric investigation whereby MOWSA finds the best  $f_{mean}$  result that has a 62.79%, 45.40%, 17.58%, and 8.46% increase from MOMVO, MOHTS, NSGWO, and MOCBO, respectively. The FNRT values achieved by MOWSA, MOHTS, MOCBO, NSGWO, and MOMVO are 500, 200, 400, 300, and 100, demonstrating the MOWSA improved solution diversity compared to other contrasted optimizers. PD measures outcomes according to Table 7, which reveals a better  $f_{mean}$  and FNRT result of MOCBO followed by MOWSA. At a 95% significance value, MOWSA exhibits its enhanced pure diversity behavior. Table 8 indicates the SP measure accordingly to the MOWSA  $f_{mean}$  the value reported a percentage decrease of 77.68%, 46.40%, and 32.66% from MOHTS, NSGWO, and MOCBO, respectively. The suggested MOWSA algorithm realizes the best FNRT value of 200 after MOMVO. At a 95%

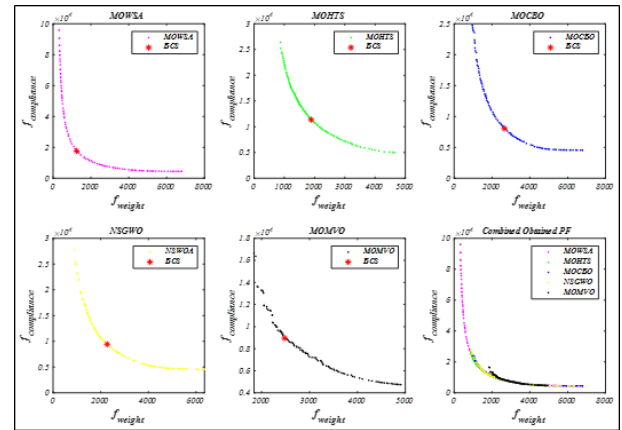


FIGURE 12. Best Pareto fronts of considered algorithms for 37-bar truss.

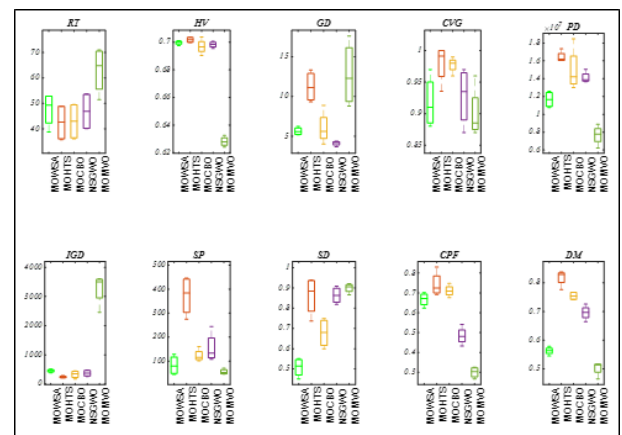


FIGURE 13. Box plots of considered algorithms for 37-bar truss.

significance value, the suggested algorithm shows a finer spacing quality behavior. Similarly, MOWSA outperforms others based on SD metric results reported in Table 9. There is a 43.52%, 41.20%, 25.06%, and 41.02% decrease reported by  $f_{mean}$  result of MOWSA concerning MOMVO, NSGWO, MOCBO, and MOHTS, respectively. MOWSA accomplished the best FNRT result of 100 and illustrated its non-dominated solutions and fair distribution against other methodologies. Referring to the IGD as specified in Table 10, MOWSA  $f_{mean}$  value realizes a significant reduction of 89.91% and 26.96% concerning the MOMVO and MOHTS algorithm. As per the FNRT test, MOWSA realizes the second-best value of 200 after MOCBO, which settled at 150. Thus, at a 95% significance value, MOWSA shows improved convergence-spread equivalence against all. Table 11 depicts the RT metric results according to which MOWSA found the best  $f_{mean}$  value reported a reduction of 32.66%, 10.74%, and 9.39% concerning MOMVO, MOHTS, and NSGWO, respectively. The MOWSA, MOHTS, MOCBO, NSGWO, and MOMVO achieve the best FNRT values of 100, 325, 200, 375, and 500, correspondingly manifest the MOWSA excellence in reaching the optimal solution with minimum computational complexity against other optimizers. As can be available from Table 12, MOWSA has the most acceptable

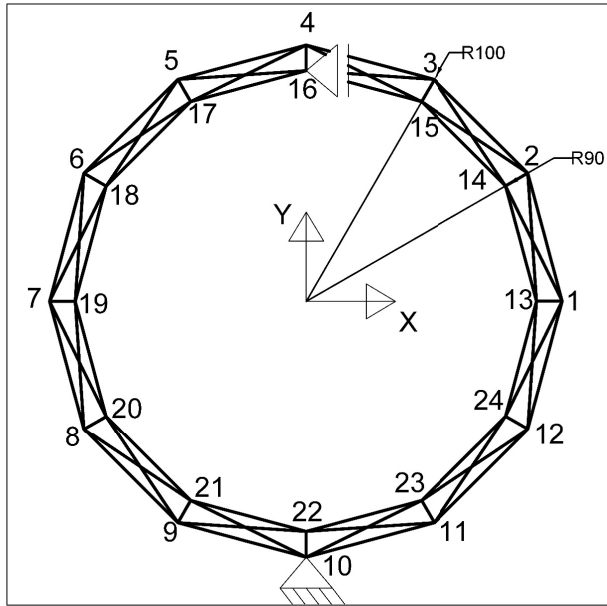


FIGURE 14. The 60-bar ring truss.

BCS results, i.e., (1244.4363, 17721.946), than any other algorithms tested.

The qualitative behavior of all considered algorithms is illustrated through their corresponding best Pareto fronts and combined behavior, as shown in Figure 12. Per comparative analysis, MOWSA provides smooth, continuous, and diverse solutions. Box plots were constructed to demonstrate the quantitative behavior of considered algorithms in terms of the performance measure (as shown in Figure 13), which depicts the superior behavior of MOWSA concerning other optimizers.

4) 60-BAR 3D TRUSS BENCHMARK

Figure 14 shows a 60-bar truss structure. The HV performance is shown in Table 2, according to which the MOHTS optimizer realizes the best  $f_{mean}$  value followed by NSGWO and MOWSA. The FNRT results accomplished by MOWSA, MOHTS, MOCBO, NSGWO, and MOMVO are 300,475,200,400, and 125, respectively. At a 95% significance value, MOWSA demonstrates its improved solutions density near the Pareto Front. GD metric is the second efficiency measure that computational results are illustrated in Table 3 accordingly MOWSA  $f_{mean}$  value presents a percentage decrease of 80.26%, 48.76%, and 46.69% from MOCBO, MOMVO, and NSGWO, respectively. MOWSA realizes the second-best FNRT value of 175 after MOHTS, revealing its convergence behavior excellence regarding MOCBO, MOMVO, and NSGWO algorithms. As per Table 4, the best CVG metric  $f_{mean}$  the result is reported by MOWSA presents a percentage decrease of 32.56%, 32.56%, 31.53%, and 30.83% from MOCBO, NSGWO, MOMVO, and MOHTS. The FNRT results accomplished by MOWSA, MOHTS, MOCBO, NSGWO, and MOMVO are 100, 275, 412.5, 412.5, and 300,

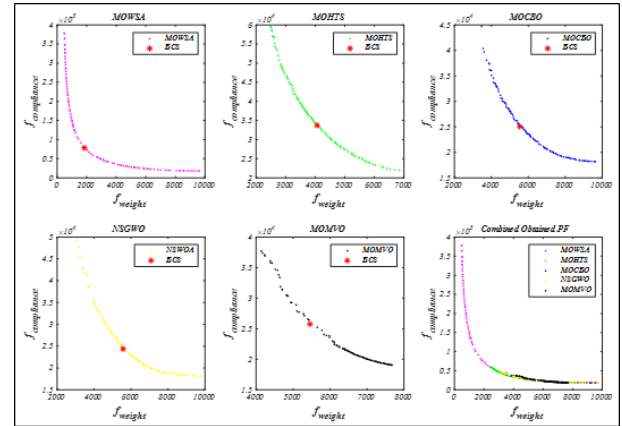


FIGURE 15. Best Pareto fronts of considered algorithms for 60-bar truss.

respectively. At a 95% significance value, MOWSA shows its improved coverage characteristic as regards other optimization strategies. Table 5 presents the CPF metric outcomes that illustrate the MOWSA realizes the best  $f_{mean}$  value that exhibits a percentage increase of 130.70%, 26.16%, and 9.12% from MOMVO, NSGWO, and MOCBO, respectively. Moreover, MOWSA found the best FNRT value of 425, followed by MOHTS, MOCBO, NSGWO, and MOMVO, which manifests its enhanced coverage over the Pareto Front feature, referring to others. DM metric computational analysis, as stated in Table 6, shows that the best  $f_{mean}$  value is realized by NSGWO that MOCBO and MOWSA succeed. The FNRT value gained by NSGWO, MOCBO, MOWSA, MOHTS, and MOMVO is 425,400,375,200, and 100, respectively. At a 95% significance value, MOWSA exhibits improved solution diversity. The PD performance measure results are illustrated in Table 7, whereby the best  $f_{mean}$  and  $f_{std}$  value is reported by the NSGWO technique. The FNRT values accomplished by MOWSA, MOHTS, MOCBO, NSGWO, and MOMVO are 350, 400, 175, 425, and 150, respectively. At a 95% significance value, MOWSA demonstrates an improved solution with pure diversity attributes. Table 8 governs the SP metric results that demonstrate  $f_{mean}$  value of the MOWSA has a substantial percentage decrease of 87.82%, 60.05%, 58.53%, and 38.75% from MOHTS, MOMVO, MOCBO, and NSGWO, respectively. Moreover,  $f_{std}$  value of MOWSA reported a substantial reduction of 70.52%, 53.33%, 44.91%, and 94.54% from MOMVO, NSGWO, MOCBO, and MOHTS algorithms, respectively. The MOWSA realizes the best FNRT value of 175 and relatively presents its optimal spacing feature. SD performance measure outcomes, as depicted in Table 9, indicate that the best  $f_{mean}$  value, i.e., 0.56910177, is attained by MOWSA that shows a 44.79%, 39.64%, 37.30%, and 43.59% decrease from MOMVO, NSGWO, MOCBO, MOHTS, respectively. The FNRT results of MOWSA, MOHTS, MOCBO, NSGWO, and MOMVO are 100,400,225,300, and 475, respectively. These findings manifest the well-distribution of MOWSA-nondominated solutions relative to others. As per the IGD metric



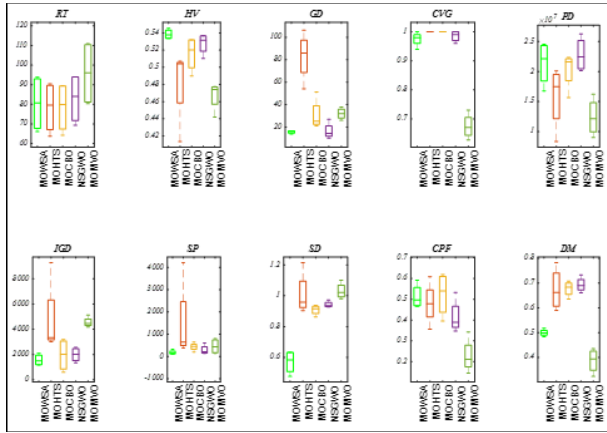


FIGURE 16. Box plots of considered algorithms for 60-bar truss.

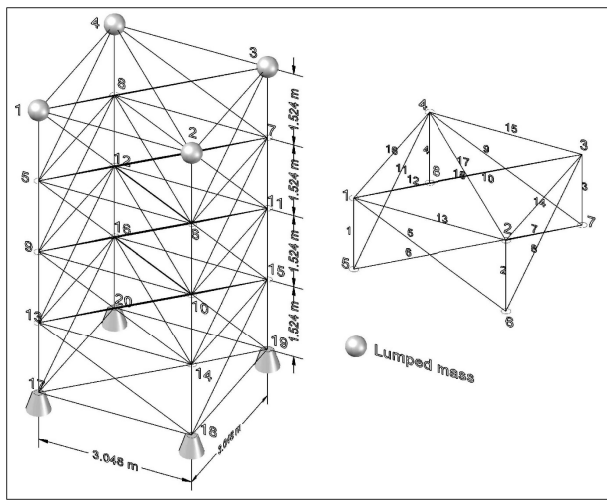


FIGURE 17. The 72-bar 3D truss.

computational analysis that is illustrated in Table 10, the leading  $f_{mean}$  and  $f_{std}$  results are exhibited MOWSA succeeds that. The FNRT results of MOWSA, MOHTS, MOCBO, NSGWO, and MOMVO are 200, 175, 425, 225, and 475, respectively, and at a 95% significance value, MOWSA demonstrates it strengthens the property of convergence-spread equivalence relatively. Table 11 indicates the RT metric results as per the best  $f_{mean}$  value of 78.3537122 reported by MOWSA, which is less than other contrasted optimization techniques. The FNRT results of MOWSA, MOHTS, MOCBO, NSGWO, and MOMVO are 120, 250, 200, 400, and 500, respectively. At a 95% significance value, MOWSA portrays its dominance in terms of the least computational time to find the optimal solutions relatively. According to Table 12, the proposed MOWSA realizes the  $f_{weight}$  value of 1852.5902 and 78036.883 value for  $f_{compliance}$  That is the best BCS among all.

Figure 15 illustrates the qualitative behavior of all five algorithms in terms of their best Pareto fronts and corresponding BCS results. Moreover, the figure presents the comparative analysis through combined Pareto fronts according to which the MOWSA solutions are well spread,

continuous, and smooth. The quantitative superiority of MOWSA over the other MHs is depicted in Figure 16 for all examined performance metric implications.

### 5) 72-BAR 3D TRUSS BENCHMARK

The 72-bar 3D truss is shown in Figure 17. According to Table 2, the best  $f_{mean}$  and  $f_{std}$  result of the HV metric is realized by MOHTS accompanied by NSGWO and MOWSA. According to FNRT analysis, the proposed MOWSA methodology achieved 400 ranks, and at a 95% significance value, it demonstrates refined solutions density near the Pareto Front. For GD indicator based on Table 3 MOWSA  $f_{mean}$  value illustrates a significant 69.45%, 53.02%, 40.02%, and 24.76% decrease from MOCBO, MOMVO, NSGWO, and MOHTS, respectively. The FNRT results of MOWSA, MOHTS, MOCBO, NSGWO, and MOMVO are 125, 275, 450, 250, and 400, respectively. These outcomes illustrate the MOWSA enhanced convergence attribute concerning other optimizers. In terms of CVG performance measures, as per Table 4, the MOWSA optimizer outperforms others by realizing the best  $f_{mean}$  and FNRT results of 0.8 and 150, respectively. Also, at a 95% significance value, MOWSA displays enhanced coverage characteristics among other algorithms. Table 5 depicts that the MOWSA CPF metric  $f_{mean}$  result has a significant percentage increase of 171.69% and 43.55% from MOMVO and NSGWO at superior  $f_{std}$  value. Moreover, MOWSA realizes the best FNRT value of 450, revealing its improved coverage over the Pareto Front attribute. Table 6 presents the DM metric investigation whereby MOWSA finds the best  $f_{mean}$  the result that has a 108.52%, 70.23%, 24.58%, and 10.53% increase from MOMVO, MOHTS, NSGWO, and MOCBO, respectively. The FNRT value achieved by MOWSA, MOHTS, MOCBO, NSGWO, and MOMVO is 500, 200, 400,300, and 100, demonstrating the MOWSA improved solution diversity compared to other contrasted optimizers. PD measures outcomes according to Table 7, which reveals a better  $f_{mean}$  of investigated.

MOWSA has a percentage increase of 84.73%, 39.64%, 22.02%, 9.30% from MOMVO, MOCBO, MOHTS, and NSGWO, correspondingly. MOWSA finds the best FNRT value of 450 out of all the optimization techniques, followed by NSGWO. At a 95% significance value, MOWSA exhibits its enhanced pure diversity behavior. Table 8 indicates the SP measure accordingly to the MOWSA  $f_{mean}$  the value stated reduction of 65.26%, 51.37%, and 5.13% from MOHTS, MOCBO, and NSGWO, respectively. The suggested MOWSA algorithm realizes the best FNRT value of 225 after MOMVO. At a 95% significance value, the suggested MOWSA shows a more acceptable spacing quality behavior. Similarly, MOWSA outperforms others based on SD metric results reported in Table 9. There is a 40.79%, 38.01%, 22.74%, and 36.64% decrease reported by  $f_{mean}$  result of MOWSA concerning MOMVO, NSGWO, MOCBO, and MOHTS, respectively. MOWSA accomplished the best FNRT result of 100 and illustrated

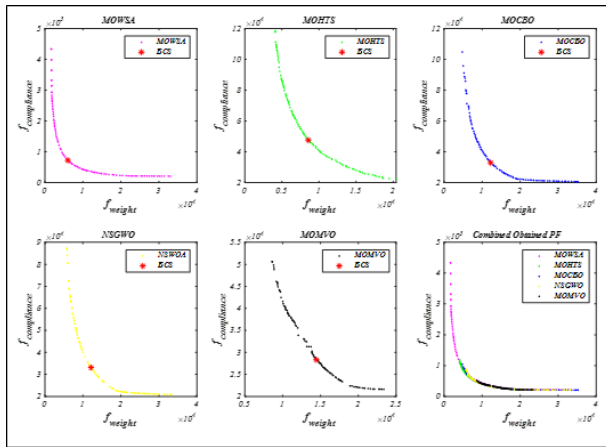


FIGURE 18. Best Pareto fronts of considered algorithms for 72-bar truss.

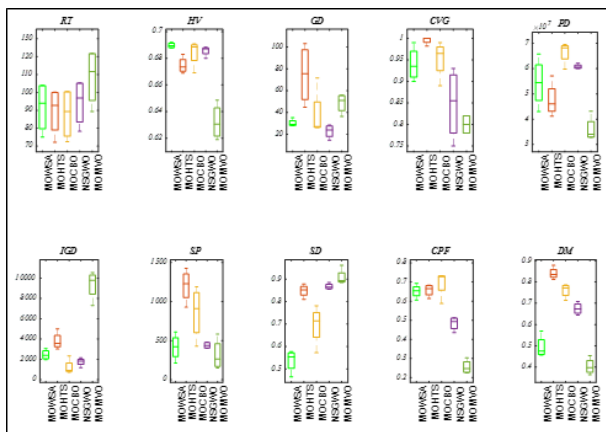


FIGURE 19. Box plots of considered algorithms for 72-bar truss.

its nondominated solution's fair distribution against other methodologies. Referring to the IGD test as indicated in Table 10, MOWSA  $f_{mean}$  value realize a significant percentage decrease of 86.89%, 67.60%, 49.80%, and 29.68% concerning MOMVO, MOCBO, MOHTS, and NSGWO algorithm. As per the FNRT test, MOWSA realizes the superior value of 150, followed by NSGWO, which settled at 175 values. Thus, at a 95% significance value, MOWSA displays its enhanced convergence-spread equivalence against all. Table 11 depicts the RT metric results according to which MOWSA found the best  $f_{mean}$  the value reported a percentage decrease of 17.67%, 5.16%, and 2.51% concerning MOMVO, NSGWA, and MOHTS, respectively. The MOWSA, MOHTS, MOCBO, NSGWA, and MOMVO achieve the best FNRT values of 150, 275, 175, 400, and 500, correspondingly manifesting the MOWSA excellence in reaching the optimal solution with minimum computational complexity against other optimizers. From BCS analysis, as can be seen in Table 12, MOWSA realizes the minimum  $f_{weight}$  results of 6046.4369 and maximum  $f_{compliance}$  value of 72102.582 amongst the other algorithms tested.

The qualitative behavior of all considered algorithms is illustrated through their corresponding best Pareto fronts and

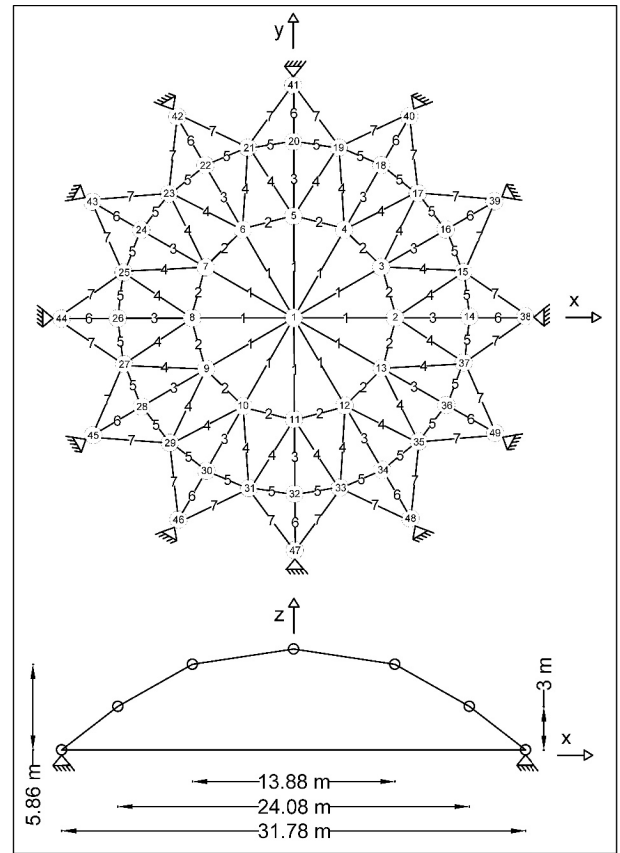


FIGURE 20. The 120-bar 3D truss.

combined behavior, as shown in Figure 18. Per comparative analysis, MOWSA provides smooth, continuous, and diverse solutions. Box plots were constructed to demonstrate the quantitative behavior of considered algorithms in terms of the performance measure (as shown in Figure 19), which depict the superior behavior of MOWSA to other optimizers.

### 6) 120-BAR 3D TRUSS BENCHMARK

The 120-bar 3D truss is shown in Figure 20. The HV efficiency measurement results are shown in Table 2, according to which the proposed MOWSA optimizer realizes the best  $f_{mean}$  value of 0.55412256. In contrast, the least  $f_{std}$  value is achieved by NSGWO. The FNRT results accomplished by MOWSA, MOHTS, MOCBO, NSGWO, and MOMVO are 475, 425, 200,300, and 100, respectively. At a 95% significance value, MOWSA displays its enhanced solutions density near the Pareto Front. GD metric is the second efficiency measure that computational results are illustrated in Table 3; accordingly, MOWSA obtains the best  $f_{mean}$  value that has a decrease of 48.58%, 41.58%, and 37.94% from MOMVO, MOCBO, and MOHTS, respectively. Also, the  $f_{std}$  value obtained by MOWSA presents a percentage decrease of 83.87%, 77.50%, 56.82%, and 39.44% concerning MOMVO, MOHTS, MOCBO, and NSGWO, respectively. MOWSA realizes the second-best FNRT value of 175 after NSGWO, revealing its convergence

behavior excellence at a 95% significance value regarding other examined algorithms. As per Table 4, the best CVG metric  $f_{mean}$  and  $f_{std}$  result is reported by the MOMVO algorithm. The FNRT results accomplished by MOWSA, MOHTS, MOCBO, NSGWO, and MOMVO are 387.5, 250, 450, 312.5, and 100, respectively. Table 5 presents the CPF metric outcomes that illustrate the MOWSA realizes the best  $f_{mean}$  the value exhibits a percentage increase of 8.87%, 84.10%, and 7.08% from MOMVO, NSGWO, and MOCBO, respectively. Moreover, MOWSA found the best FNRT value of 475, followed by MOHTS, which manifests its enhanced coverage over the Pareto Front feature, referring to others. DM metric computational analysis, as stated in Table 6, shows that the best  $f_{mean}$  value is realized by MOWSA, which has an increase of 29.80%, 33.06%, 12.24%, and 40.64% from MOMVO, NSGWO, MOCBO, and MOHTS algorithms correspondingly. The FNRT values gained by MOWSA, MOHTS, MOCBO, NSGWO, and MOMVO are 500, 125, 400, 225, and 250, respectively. At 95% significance value, MOWSA exhibits improved solution diversity. The PD performance measure results are shown in Table 7, whereby the best  $f_{mean}$  is accomplished by the MOWSA technique and displays a percentage increase of 68.09%, 13.18%, 37.91%, and 31.39% from MOMVO, NSGWO, MOCBO, and MOHTS, respectively. The FNRT values accomplished by MOWSA, MOHTS, MOCBO, NSGWO, and MOMVO are 475, 275, 200, 375, and 175, respectively. At 95% significance value, MOWSA demonstrates an enhanced solution with pure diversity attributes over other algorithms. Table 8 governs the SP metric results that demonstrate  $f_{mean}$  value of the MOWSA has a substantial percentage decrease of 86.51%, 73.50%, 64.39%, and 55.28% from MOHTS, MOMVO, MOCBO, and NSGWO, respectively. Moreover,  $f_{std}$  value of MOWSA reported a significant decrease of 97.29%, 95.39%, 86.08%, and 77.12% from MOMVO, MOHTS, MOCBO, and NSGWO, respectively. The MOWSA realizes the best FNRT value of 100 and relatively presents its optimal spacing feature. SD performance measure outcomes, as depicted in Table 9, indicates that the best  $f_{mean}$  value, i.e., 0.20310314, is attained by MOWSA, showing a substantial 79.32%, 79.22%, 69.70%, and 77.70% decrease from MOMVO NSGWO, MOCBO, and MOHTS, respectively. The FNRT results of MOWSA, MOHTS, MOCBO, NSGWO, and MOMVO are 100, 300, 200, 450, and 450, respectively. These findings manifest the well-distribution of MOWSA non-dominated solutions relative to others. As per the IGD metric computational analysis that is illustrated in Table 10, the leading  $f_{mean}$  and  $f_{std}$  results are exhibited by the MOHTS technique that MOWSA succeeds. The FNRT results of MOWSA, MOHTS, MOCBO, NSGWO, and MOMVO are 175, 125, 350, 350, and 500, respectively; MOWSA demonstrates its strength in the property of convergence-spread equivalence relatively. Table 11 indicates the RT metric results according to which best  $f_{mean}$  value of is reported by MOCBO while the  $f_{std}$  results of MOWSA are less than other contrasted

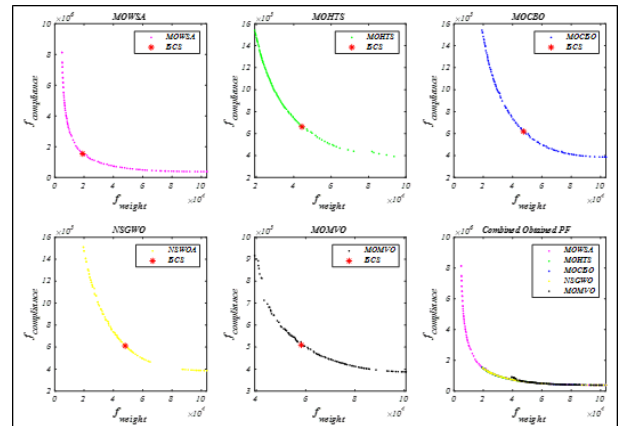


FIGURE 21. Best Pareto fronts of considered algorithms for 120-bar truss.

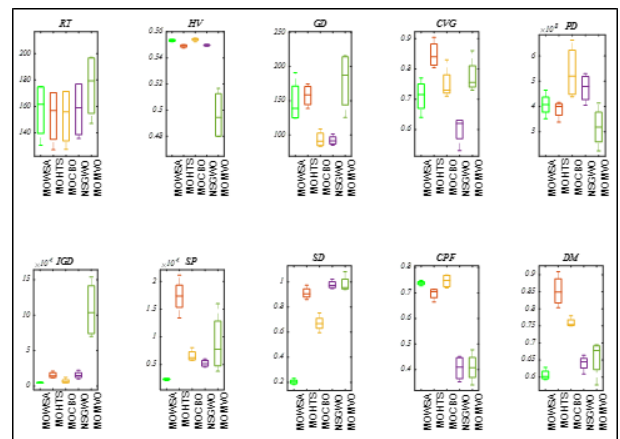


FIGURE 22. Box plots of considered algorithms for 120-bar truss.

optimization techniques. The FNRT results of MOWSA, MOHTS, MOCBO, NSGWO, and MOMVO are 150, 325, 175, 350, and 500, respectively. At a 95% significance value, MOWSA portrays its dominance in terms of the minimum computational cost to find the optimal solutions relatively. According to Table 12, the proposed MOWSA realizes the  $f_{weight}$  value of 19060.176 and 1546234.8 value for  $f_{compliance}$  That is the best BCS among all.

Figure 21 illustrates the qualitative behavior of all five algorithms in terms of their best Pareto fronts and corresponding BCS results. Moreover, the figure presents the comparative analysis through combined Pareto fronts according to which the MOWSA solutions are well spread, continuous, and smooth. The quantitative superiority of the proposed MOWSA technique over the others is depicted in Figure 22 for all examined performance metric implications.

### 7) 200-BAR 3D TRUSS BENCHMARK

The 200-bar 3D truss structure is shown in Figure 23. According to Table 2, the best  $f_{mean}$  and  $f_{std}$  result of the HV metric is realized by MOCBO accompanied by NSGWO and MOWSA. According to FNRT analysis, the proposed MOWSA methodology achieved 325 ranks, and at a 95% significance value, it demonstrates refined solutions density near the Pareto Front. For GD indicator based on Table 3



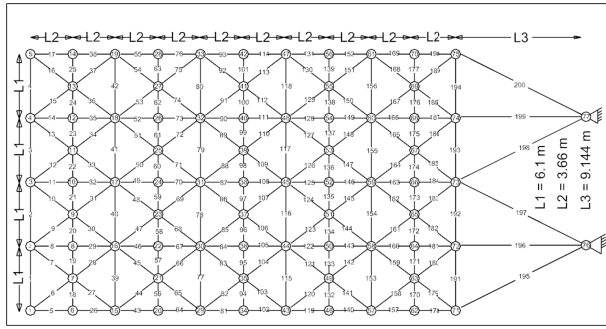


FIGURE 23. The 200-bar 3D truss.

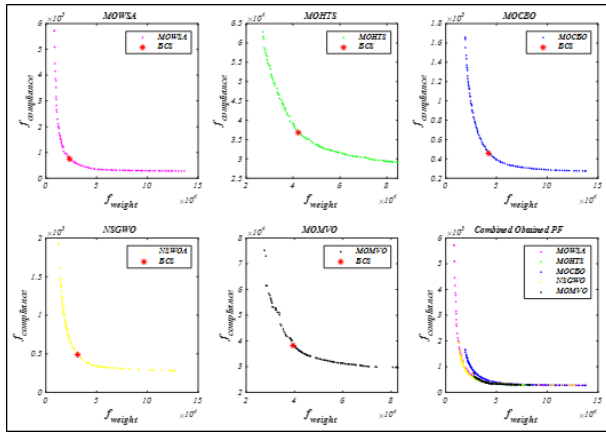


FIGURE 24. Best Pareto fronts of considered algorithms for 200-bar truss.

MOHTS  $f_{mean}$  value is the best, while the MOMVO reported the least  $f_{std}$  result relatively. The FNRT results of MOWSA, MOHTS, MOCBO, NSGWO, and MOMVO are 250, 125, 450, 400, and 275, respectively. These outcomes illustrate the MOWSA enhanced convergence attribute regarding other optimizers at a degree of 95% significance. In terms of CVG performance measures as per Table 4, the MOWSA optimizer outperforms others by realizing the best  $f_{mean}$  and FNRT results of 0.6825 and 100, respectively. Also, at a 95% significance value, MOWSA displays enhanced coverage characteristics among other algorithms. Table 5 depicts that the MOWSA CPF metric  $f_{mean}$  the result has a significant percentage increase of 254.02%, 75.50%, and 68.79% from MOMVO, NSGWO, and MOHTS at better  $f_{std}$  value. The FNRT results of MOWSA, MOHTS, MOCBO, NSGWO, and MOMVO are 400, 225, 500, 275, and 100, respectively. At a 95% significance value, MOWSA reveals its enhanced coverage over the Pareto Front attribute. Table 6 presents the DM metric investigation whereby MOWSA finds the best  $f_{mean}$  result with a 133.09%, 56.94%, and 35.53% increase from MOMVO, MOHTS, and NSGWO. Here, MOCBO finds the least  $f_{std}$  value. The FNRT values achieved by MOWSA, MOHTS, MOCBO, NSGWO, and MOMVO are 450, 225, 450, 275, and 100, demonstrating the MOWSA improved solution diversity compared to other contrasted optimizers. PD measure outcomes according to Table 7, which reveals a better  $f_{mean}$  of investigated MOWSA has a percentage increase of 149.61%, 105.34%, 20.20%, and

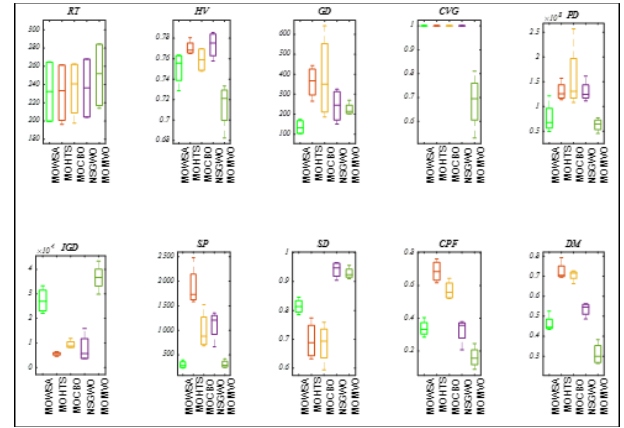


FIGURE 25. Box plots of considered algorithms for 200-bar truss.

22.13% from MOMVO, MOHTS, NSGWO, and MOCBO correspondingly. MOWSA finds the best FNRT value of 425 out of all the optimization techniques considered, followed by MOCBO. At 95% significance value, MOWSA exhibits its enhanced pure diversity behavior. Table 8 indicates the SP measure accordingly to the MOWSA  $f_{mean}$  the value reported a percentage decrease of 84.06%, 72.95%, and 69.71% from MOHTS, NSGWO, and MOCBO, respectively. Likewise, MOWSA achieves the best the  $f_{std}$  result that realizes an 81.92%, 80.69%, and 75.71% decrease over MOHTS, MOCBO, and NSGWO, respectively. MOWSA and MOMVO algorithms realize the best FNRT value of 150. At a 95% significance value, the suggested MOWSA shows a more acceptable spacing quality behavior against other techniques. MOCBO outperforms others based on the SD metric  $f_{mean}$  results are reported in Table 9. The MOWSA, MOHTS, MOCBO, NSGWA, and MOMVO achieve FNRT values of 300, 150, 150, 475, and 425, respectively. Thus, MOWSA illustrates its non-dominated solutions' fair distribution against other methodologies at a degree of 95% significance. Referring to the IGD test as specified in Table 10, MOCBO finds the best  $f_{mean}$  and  $f_{std}$  value. The FNRT results of MOWSA, MOHTS, MOCBO, NSGWO, and MOMVO are 275, 425, 150, 175, and 475. Thus, at a 95% significance value, MOWSA displays its enhanced convergencespread equivalence. Table 11 depicts the RT metric results according to which MOWSA found the best  $f_{mean}$  and  $f_{std}$  results relative to other accounted optimization techniques. The MOWSA, MOHTS, MOCBO, NSGWA, and MOMVO achieve the best FNRT values of 150, 250, 250, 350, and 500 correspondingly, manifesting the MOWSA excellence in reaching the optimal solution with minimum computational complexity against other optimizers. From BCS analysis, as can be seen in Table 12, MOWSA realizes the minimum  $f_{weight}$  results of 23201.131 and maximum  $f_{compliance}$  value of 74750.126 amongst other algorithms tested.

The qualitative behavior of all considered algorithms is illustrated through their corresponding best Pareto fronts and combined behavior, as shown in Figure 24. Per comparative



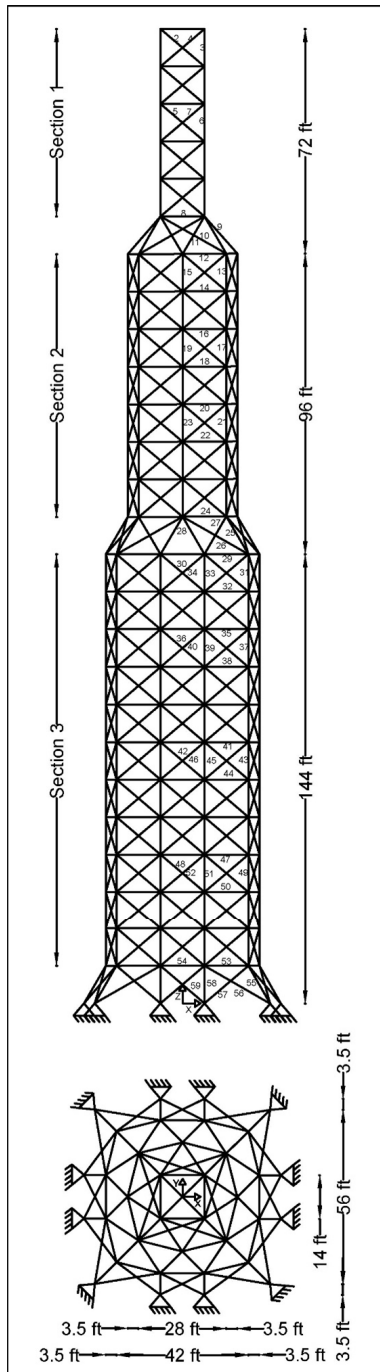


FIGURE 26. The 942-bar tower truss.

analysis, MOWSA provides smooth, continuous, and diverse solutions. Box plots were constructed to demonstrate the quantitative behavior of considered algorithms in terms of the performance measure (as shown in Figure 25), which depict the superior behavior of MOWSA with other optimizers.

#### 8) 942-BAR 3D TRUSS BENCHMARK

Figure 26 shows a 942-bar tower truss. The HV performance measure results are depicted in Table 2, according to which the MOCBO optimizer realizes the best  $f_{\text{mean}}$

value of 0.72003647 succeeded by NSGWO and MOWSA that realized the nearly identical result. The FNRT results accomplished by MOWSA, MOHTS, MOCBO, NSGWO, and MOMVO are 325, 225, 425, 375, and 150, respectively. At a 95% significance value, MOWSA demonstrates its improved solutions density near the Pareto Front. GD metric is the second efficiency measure that computational results are illustrated in Table 3; accordingly, NSGWO finds the best  $f_{\text{mean}}$  result whereas the best  $f_{\text{std}}$  value is exhibited by MOHTS. MOHTS realizes the best FNRT value followed by MOMVO, revealing its convergence behavior excellence regarding other examined algorithms. As per Table 4, the best CVG metric  $f_{\text{mean}}$  result is reported by the MOWSA algorithm. The FNRT results accomplished by MOWSA, MOHTS, MOCBO, NSGWO, and MOMVO are 100, 275, 375, 375, and 375, respectively. Hence, at a 95% significance value, MOWSA shows improved coverage characteristics among other algorithms. Table 5 presents the CPF metric outcomes that illustrate the MOCBO realizes the best  $f_{\text{mean}}$  value. Moreover, MOWSA found the second-best FNRT value of 375 after MOCBO, manifesting its enhanced coverage over the Pareto Front feature. DM metric computational analysis, as stated in Table 6, shows that the best  $f_{\text{mean}}$  value is realized by MOWSA, which has a percentage increase of 291.16%, 88.43%, 41.64%, and 31.35% from MOMVO, MOHTS, NSGWO, and MOCBO algorithms correspondingly. The FNRT values gained by MOWSA, MOHTS, MOCBO, NSGWO, and MOMVO are 500, 200, 350, 350, and 100, respectively. At a 95% significance value, MOWSA exhibits improved solution diversity compared to others. The PD performance measure results are shown in Table 7, whereby the best  $f_{\text{mean}}$  is accomplished by the MOCBO technique. The FNRT values accomplished by MOWSA, MOHTS, MOCBO, NSGWO, and MOMVO are 375, 200, 425, 400, and 100, respectively. At 95% significance value, MOWSA demonstrates an improved solution pure diversity attribute. Table 8 governs the SP metric results that demonstrate  $f_{\text{mean}}$  value of the MOWSA has a substantial percentage decrease of 68.40%, 65.85%, and 55.45% from MOHTS, NSGWO, MOCBO, respectively. Moreover,  $f_{\text{std}}$  value of MOWSA reported a major 69.73%, 63.53%, and 37.90% decrease from MOHTS, NSGWO, and MOCBO, respectively. The MOWSA realizes the best FNRT value of 150, which relatively presents its optimal spacing feature. SD performance measure outcomes, as depicted in Table 9, indicate that the best  $f_{\text{mean}}$  value is attained by MOHTS, succeeded by MOWSA. The FNRT results of MOWSA, MOHTS, MOCBO, NSGWO, and MOMVO are 250, 100, 275, 425, and 450, respectively. These findings manifest the well-distribution of MOWSA's non-dominated solutions. As per the IGD metric computational analysis that is illustrated in Table 10, the leading  $f_{\text{mean}}$  and  $f_{\text{std}}$  results are exhibited by the MOCBO technique that NSGWO succeeds. The FNRT results of MOWSA, MOHTS, MOCBO, NSGWO, and MOMVO are 275, 400, 150, 175, 500, respectively, and at a 95% significance value, MOWSA reveals

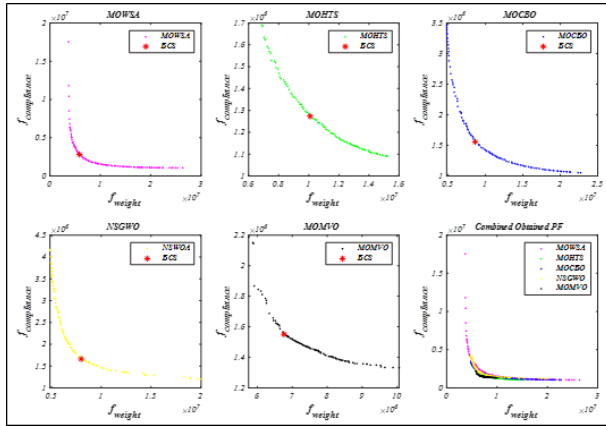


FIGURE 27. Best Pareto fronts of considered algorithms for 942-bar truss.

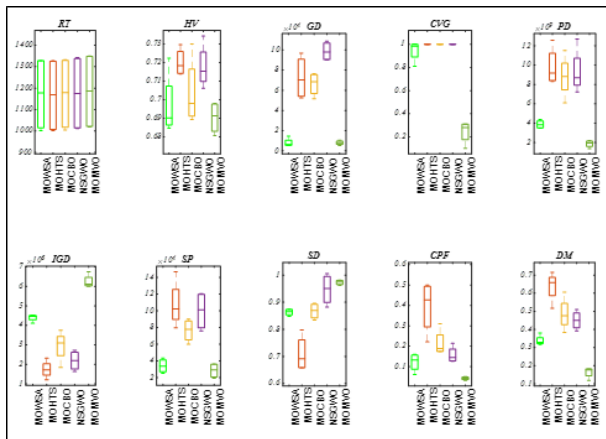


FIGURE 28. Box plots of considered algorithms for 942-bar truss.

its enhanced property of convergence-spread equivalence. Table 11 indicates the RT metric results as per the best  $f_{mean}$  value of is reported by the proposed MOWSA. The FNRT results of MOWSA, MOHTS, MOCBO, NSGWO, and MOMVO are 125, 275, 325, 325, and 450, respectively. At a 95% significance value, MOWSA portrays its dominance in terms of the least computational time to find the optimal solutions relatively. According to Table 12, the proposed MOWSA realizes the  $f_{weight}$  value of 5857383.8 and 2802136.4 value for  $f_{compliance}$ , that is the best BCS among all.

Figure 27 illustrates the qualitative behavior of all five algorithms in terms of their best Pareto fronts and corresponding BCS results. Moreover, the figure presents the comparative analysis through combined Pareto fronts according to which the MOWSA solutions are well spread, continuous, and smooth. The quantitative superiority of the proposed MOWSA technique over others is depicted in Figure 28 for all examined performance metric implications.

To make all computational analysis comprehensive, the average FNRT value of each metric is illustrated at the end of the respective tables, along with the ranking. For the SD measure, as depicted in Table 2, MOWSA exhibited the maximum average value of 3100 and achieved the first ranking, followed by MOHTS. MOWSA finds the least

average GD metric value of 1550 and ranked first amongst all, as depicted in Table 3. Regarding the CVG metric, as shown in Table 4, the best average value is realized by MOMVO, i.e., 1762.5, while MOWSA settled at second rank with a 1837.5 value. MOWSA finds the maximum average value of 3550 for the CPF metric as per Table 5 and ranked first, followed by MOCBO. Regarding the DM metric average FNRT value (refer to Table 6), MOWSA reports a maximum result of 3825 and is ranked first. Similarly, for the PD metric (as shown in Table 7), the maximum result is exhibited by MOWSA, i.e., 3300, which makes it rank first, succeeded by NSGWO. In the context of the SP metric, as illustrated in Table 8, the least average FNRT value of 1225 is realized by MOWSA, while MOMVO accomplishes the second rank. From Table 9, it is evident that the minimum value of 1150 is obtained by MOWSA and ranked first, while MOCBO achieved the second position. The IGD measure (as demonstrated in Table 10) shows the first ranking of MOWSA owing to its least 1550 average FNRT value. Both MOHTS and NSGWO ranked second with the same 2125 mean value. In terms of crucial RT metric as illustrated in Table 11, suggested MOWSA found the first rank with the least value of 1050, succeeded by MOCBO. Also, it is evident from Table 12 that MOWSA found the best BCS results for all considered 2D and 3D benchmarks. Therefore, the aforementioned computational analysis and discussions demonstrate that the proposed MOWSA optimization methodology outperforms others in resolving real-world complex structural optimization problems and has a balanced trade-off between exploration and exploitation of search.

The Multi-objective Water Strider Algorithm (MOWSA), a novel approach utilizing an elitist non-dominated sorting mechanism and crowding distance to optimize complex truss structures. Our empirical evaluation demonstrates MOWSA’s notable efficacy, outperforming established algorithms like MOHTS, NSGWO, MOCBO, and MOMVO. This superiority is attributed to MOWSA’s unique balance between exploration and exploitation abilities, as evidenced by its performance metrics across various truss test cases. Particularly, the algorithm’s adeptness in navigating the multi-dimensional search space, as seen in its Hypervolume (HV) and Inverted-Generational Difference (IGD) scores, highlights its proficiency in achieving a diverse set of Pareto-optimal solutions. However, our analysis extends beyond mere performance metrics. We delve into the algorithm’s structural nuances, examining how its components contribute to its effectiveness. For instance, integrating a crowding distance mechanism ensures solution diversity, a crucial factor in multi-objective optimization.

**C. EXPERIMENTAL RESULTS ON LARGE SCALE OPTIMIZATION BENCHMARK PROBLEMS (LSMOP1-LSMOP9)**

Table 13 presents the Generational Distance (GD) results for MOWSA, MOHTS, MOCBO, NSGWO, MOMVO, and

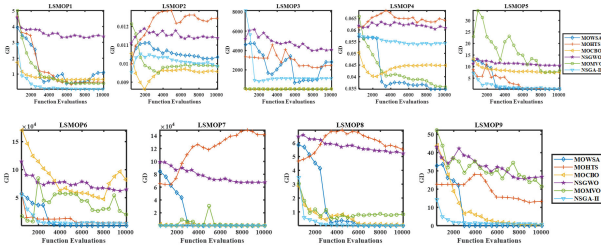


**FIGURE 29.** Convergence curve of GD metric on state of the art algorithms for LSMOP1-LSMOP9 problems.

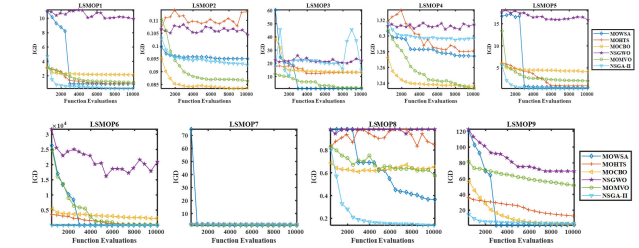


**FIGURE 31.** Convergence curve of GD metric on state of the art algorithms for LSMOP1-LSMOP9 problems.

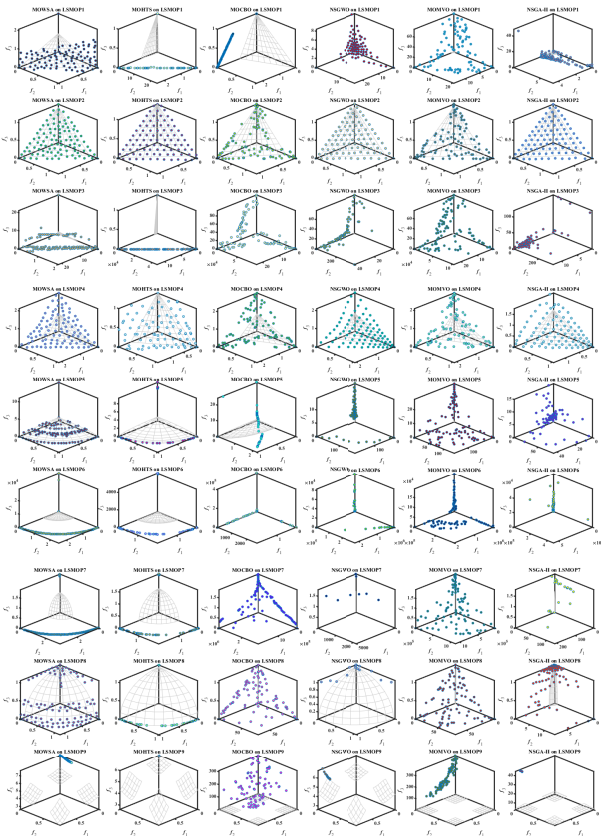


**FIGURE 30.** Pareto fronts of state of the art algorithms for LSMOP1-LSMOP9 problems.

NSGA-II on LSMOP test problems. For problem LSMOP1 with 3-M and 300-D, MOWSA records a mean GD of  $1.1038e+0$  ( $4.57e-1$ ), which is significantly better than NSGA-II with  $5.7770e-2$  ( $6.43e-2$ ), and competitive with MOMVO which shows a GD of  $4.2015e-1$  ( $1.10e-1$ ). In LSMOP3 with the same 3-M and 300-D configuration, MOWSA has a mean GD of  $2.8136e+3$  ( $1.23e+2$ ), outperforming NSGA-II which has a GD of  $1.1315e+3$  ( $1.96e+3$ ) and closely following NSGWO with a GD of  $4.0939e+3$  ( $8.25e+2$ ). The table indicates that MOWSA is a competitive algorithm across the LSMOP test suite, often achieving lower mean GD values, indicating a closer approximation to the true Pareto front, signifying better performance. MOWSA particularly excels in LSMOP6 with a mean GD of  $1.3024e+2$  ( $6.20e+0$ ), showcasing its effectiveness in

dealing with complex many-objective optimization problems, as compared to NSGA-II which records a higher mean GD of  $4.1721e+3$  ( $3.43e+3$ ). Across the LSMOP test suite, MOWSA's performance ranges from competitive to superior, as it achieves better results in many cases when compared to the other algorithms shown in Fig. 29. For instance, in LSMOP2, MOWSA achieves a mean GD of  $1.0350e-2$  ( $1.12e-4$ ), which is better than NSGA-II's  $9.8584e-3$  ( $3.78e-4$ ). A lower mean GD indicates a closer approximation to the true Pareto front shown in Fig. 30, signifying better performance of the MOWSA algorithm. Such results highlight the robustness of MOWSA in navigating the trade-offs inherent in large-scale multi-objective optimization tasks.

Table 14 presents the Inverted Generational Distance (IGD) results for MOWSA, among other algorithms, on LSMOP test problems. MOWSA demonstrates competitive performance compared to its counterparts, with notable success across various problem instances. In LSMOP1 with 3 objectives (M) and 300 decision variables (D), MOWSA achieves a mean IGD of  $8.6071e-1$  ( $\pm 1.20e-5$ ), which is considerably better than NSGA-II which records  $2.1304e-1$  ( $\pm 3.64e-2$ ). This performance indicates MOWSA's robustness and effective convergence to the Pareto front. Across the LSMOP test suite, MOWSA frequently achieves lower mean IGD values, indicating a closer approximation to the true Pareto front, which signifies the efficiency of MOWSA in addressing complex many-objective optimization problems. For instance, in LSMOP6, MOWSA records a mean IGD of  $1.2670e+0$  ( $\pm 2.29e-4$ ), while NSGA-II logs  $1.2879e+0$  ( $\pm 1.92e-1$ ), demonstrating MOWSA's competitive edge. In several instances, MOWSA outperforms other algorithms concerning mean IGD values. For LSMOP2, MOWSA posts a mean IGD of  $9.5040e-2$  ( $\pm 4.64e-4$ ), outshining NSGA-II with a slightly higher mean IGD of  $9.2655e-2$  ( $\pm 1.05e-3$ ). Similarly, in LSMOP4, MOWSA's mean IGD of  $2.7429e-1$  ( $\pm 1.33e-3$ ) is better than that of NSGA-II, which is  $2.9683e-1$  ( $\pm 1.03e-3$ ). The trend of MOWSA's performance is consistent, often outperforming NSGA-II and showing competitive results against other algorithms. It is particularly noteworthy in LSMOP9, where MOWSA has a mean IGD of  $1.5379e+0$  ( $\pm 0.00e+0$ ), while NSGA-II shows  $3.3175e+0$  ( $\pm 6.43e-1$ ), highlighting the superior solution quality offered by MOWSA. Regarding the proportion of test problems where MOWSA outshines other algorithms,



TABLE 13. Results of (GD Metric) on LSMOP problems.

Algorithms	M	D	MOWSA	MOHTS	MOCBO	NSGWO	MOMVO	NSGA-II
LSMOP1	3	300	1.1038e+0 ± 4.57e-1	4.9505e-1 ± 5.88e-1	2.4190e+0 ± 3.02e+0	3.3759e+0 ± 2.48e-1	4.2015e-1 ± 1.10e-1	5.7770e-2 ± 6.43e-2
LSMOP2	3	300	1.0350e-2 ± 1.12e-4	1.2445e-2 ± 7.78e-5	9.5747e-3 ± 1.79e-4	1.1381e-2 ± 1.66e-4	9.8610e-3 ± 9.28e-4	9.8584e-3 ± 3.78e-4
LSMOP3	3	300	2.8136e+3 ± 1.23e+2	2.4818e+3 ± 2.13e+3	1.4547e+1 ± 9.31e+0	4.0939e+3 ± 8.25e+2	3.9487e+1 ± 1.64e+1	1.1315e+3 ± 1.96e+3
LSMOP4	3	300	3.4668e-2 ± 5.86e-4	6.4158e-2 ± 1.32e-3	4.4834e-2 ± 8.80e-4	6.0934e-2 ± 1.41e-3	3.5630e-2 ± 7.13e-3	5.4384e-2 ± 7.36e-4
LSMOP5	3	300	2.2379e-1 ± 2.29e-2	4.5463e-1 ± 1.40e-1	7.4879e+0 ± 5.61e-1	1.0493e+1 ± 2.17e-1	8.2493e+0 ± 7.43e+0	5.3232e-1 ± 5.17e-1
LSMOP6	3	300	1.3024e+2 ± 6.20e+0	4.7881e+3 ± 8.42e+2	8.2214e+4 ± 4.52e+4	6.4771e+4 ± 1.84e+4	2.0025e+4 ± 3.09e+4	4.1721e+3 ± 3.43e+3
LSMOP7	3	300	9.8750e-2 ± 3.90e-4	1.4174e+5 ± 2.72e+4	5.5282e+2 ± 5.81e+2	6.7565e+4 ± 9.47e+3	2.2787e+1 ± 2.63e+1	2.2324e-1 ± 2.34e-3
LSMOP8	3	300	1.9045e-3 ± 2.28e-4	5.5337e+0 ± 8.40e-1	5.9701e-2 ± 1.55e-2	5.2223e+0 ± 6.82e-1	8.2232e-1 ± 3.09e-1	1.2660e-2 ± 1.42e-3
LSMOP9	3	300	0.0000e+0 ± 0.00e+0	1.3195e+1 ± 9.33e+0	5.6958e-1 ± 3.62e-1	2.6802e+1 ± 1.40e+0	2.1437e+1 ± 8.24e+0	7.4282e-1 ± 5.42e-1

TABLE 14. Results of (IGD Metric) on LSMOP problems.

Algorithms	M	D	MOWSA	MOHTS	MOCBO	NSGWO	MOMVO	NSGA-II
LSMOP1	3	300	8.6071e-1 ± 1.20e-5	8.5705e-1 ± 3.18e-3	4.9912e+0 ± 4.96e+0	9.9490e+0 ± 6.33e-1	1.0917e+0 ± 3.23e-1	2.1304e-1 ± 3.64e-2
LSMOP2	3	300	9.5040e-2 ± 4.64e-4	1.1335e-1 ± 3.25e-3	8.3676e-2 ± 1.40e-3	1.0446e-1 ± 1.04e-3	8.6307e-2 ± 2.45e-3	9.2655e-2 ± 1.05e-3
LSMOP3	3	300	8.6072e-1 ± 1.36e-16	1.3251e+1 ± 1.11e+1	1.3163e+1 ± 2.76e-1	2.2158e+1 ± 5.84e+0	1.4254e+0 ± 9.78e-1	1.5090e+1 ± 2.18e+1
LSMOP4	3	300	2.7429e-1 ± 1.33e-3	2.8106e-1 ± 5.52e-3	2.3639e-1 ± 2.45e-3	3.1456e-1 ± 1.28e-2	2.3321e-1 ± 2.23e-2	2.9683e-1 ± 1.03e-3
LSMOP5	3	300	5.4313e-1 ± 6.19e-4	9.4592e-1 ± 0.00e+0	4.1245e+0 ± 2.11e-1	1.5893e+1 ± 1.07e+0	2.0507e+0 ± 2.32e-1	3.2621e-1 ± 1.89e-1
LSMOP6	3	300	1.2670e+0 ± 2.29e-4	2.8879e+2 ± 4.97e+2	2.2636e+3 ± 1.35e+3	2.0981e+4 ± 1.41e+4	1.8995e+2 ± 1.71e+2	1.2879e+0 ± 1.92e-1
LSMOP7	3	300	9.9772e-1 ± 7.88e-4	1.4513e+0 ± 6.17e-2	1.4323e+0 ± 1.01e-1	1.6280e+0 ± 5.78e-2	1.0400e+0 ± 1.09e-1	1.5257e+0 ± 2.06e-2
LSMOP8	3	300	3.6636e-1 ± 1.64e-3	8.4929e-1 ± 6.11e-2	6.5186e-1 ± 2.75e-2	9.8254e-1 ± 4.08e-4	5.7569e-1 ± 7.16e-2	1.3943e-1 ± 9.66e-3
LSMOP9	3	300	1.5379e+0 ± 0.00e+0	1.2708e+1 ± 5.22e+0	2.5054e+0 ± 1.08e+0	6.9495e+1 ± 3.23e+0	5.1540e+1 ± 1.17e+1	3.3175e+0 ± 6.43e-1

TABLE 15. Results of (RT Metric) on LSMOP problems.

Algorithms	M	D	MOWSA	MOHTS	MOCBO	NSGWO	MOMVO	NSGA-II
LSMOP1	3	300	3.59E+00	3.60E+01	4.55E+00	7.34E+02	5.79E+00	5.00E+00
LSMOP2	3	300	2.82E+00	5.46E+01	4.56E+00	4.02E+00	7.40E+00	5.02E+00
LSMOP3	3	300	2.80E+00	4.03E+01	4.64E+00	7.22E+00	5.33E+00	4.13E+00
LSMOP4	3	300	3.16E+00	6.42E+01	5.00E+00	4.48E+00	8.34E+00	5.33E+00
LSMOP5	3	300	2.75E+00	6.89E+01	4.23E+00	4.12E+00	4.44E+00	4.61E+00
LSMOP6	3	300	2.88E+00	4.52E+01	4.39E+00	5.73E+00	4.08E+00	4.40E+00
LSMOP7	3	300	2.90E+00	6.94E+01	4.63E+00	1.76E+01	5.74E+00	4.46E+00
LSMOP8	3	300	3.00E+00	7.15E+01	4.45E+00	7.37E+00	6.15E+00	4.86E+00
LSMOP9	3	300	2.99E+00	4.71E+01	4.89E+00	2.35E+01	4.31E+00	4.30E+00

as shown in Fig. 31, it is evident that MOWSA secures a significant number of best results in evaluating the IGD metric across the LSMOP problems. This is exemplified by LSMOP5, where MOWSA records a mean IGD of 5.4313e-1 (±6.19e-4), compared to the higher IGD value of NSGA-II which is 3.2621e-1 (±1.89e-1). Overall, the data from Table 14 suggest that MOWSA is a highly effective algorithm for many-objective optimization problems. It offers better convergence and diversity when solving LSMOP test problems, often achieving lower mean IGD values than its counterparts.

From Table 15, the overall running time of MOWSA is consistently competitive among the algorithms tested, indicating its efficient use of computational resources in solving LSMOP problems. For instance, in LSMOP1 with 3 objectives (M) and 300 decision variables (D), MOWSA has a running time of 3.59, substantially lower than NSGWO, which has a running time of 734. This demonstrates MOWSA's computational efficiency, especially compared to NSGWO, which requires much more computational time. In LSMOP7, MOWSA's running time is 2.90, while MOHTS is at 69.4, showing that MOWSA is significantly faster and, hence, can be considered more efficient in computational time. This trend is consistent across various LSMOP problems, indicating that MOWSA effectively finds

high-quality solutions and does so with a quicker runtime. Comparatively, MOWSA's running times are very close to NSGA-II across all problems, suggesting that it provides a competitive balance between performance and computational speed. In LSMOP6, MOWSA shows a running time 2.88 against NSGA-II's 4.40. This slight difference, while maintaining competitive performance, highlights MOWSA's advantage in speed efficiency. MOWSA demonstrates its superior efficiency in diverse LSMOP scenarios, often requiring less computational time than other algorithms such as MOHTS and NSGWO while maintaining a performance that is on par with or better than NSGA-II and MOMVO. For example, in LSMOP9, MOWSA's running time is recorded at 2.99, which is faster than MOMVO's time of 4.31 and almost identical to NSGA-II's time of 4.30. Therefore, it can be concluded from the experimental results in Table 15 that MOWSA exhibits a competitive running speed and demonstrates high search efficiency, making it a strong candidate for solving complex engineering optimization problems efficiently.

The provided data indicates that the MOWSA algorithm demonstrates promising performance in large-scale multi-objective optimization problems (LSMOP), as evidenced by its competitive or superior results in Generational Distance (GD) and Inverted Generational Distance (IGD) metrics



compared to established algorithms like NSGA-II, MOHTS, MOCBO, NSGWO, and MOMVO. MOWSA exhibits a closer approximation to the true Pareto front and efficient computational time, suggesting its potential in handling complex multi-objective optimization tasks. However, the critique that the paper lacks rigorous evaluation and comparison with state-of-the-art multi-objective benchmarks and algorithmic frameworks is valid.

As presented in the theory, the integration of non-dominant sorting into the Water Strider Algorithm (WSA) demonstrates effective results in various optimization scenarios, notably in solving large scale with 300 decision variables based on LSMOP and truss bar problems.

## VI. CONCLUSION

For the design and optimization of the MO truss-bar, the current research designed and deployed a unique MOWSA algorithm. The lifecycle of water strider insects is the motivation of the proposed technique mathematically formulated by imitating territorial behavior, intelligent ripple communication, mating style, feeding mechanisms, and succession of water striders. To enhance the solution quality and achieve a proper trade-off between search exploration and exploitation of NDS and CD is used in this study. The MOWSA algorithm was rigorously tested on nine large-scale multiobjective benchmark problems (LSMOP1-LSMOP9) with 300 decision variables and eight distinct structural optimization benchmarks (specifically the 10-bar, 25-bar, 37-bar, 60-bar, 72-bar, 120-bar, 200-bar, and 942-bar models) to assess its capabilities in exploration, exploitation, avoiding local optima, and convergence. This evaluation involved a comparative analysis with four renowned algorithms, utilizing ten established performance metrics. This analysis included quantitative and qualitative approaches, focusing on the non-dominated solution set, the most effective compromise solutions, and their distribution pattern near Pareto fronts. The average Friedman's rank test positioned the proposed MOWSA approach at the forefront for most technical challenges. Comprehensive examination indicates that MOWSA holds a notable edge over competing optimization tools regarding coverage, convergence, and diversity of solutions, demonstrating its effectiveness in addressing complex, large-scale, real-world optimization challenges.

While MOWSA demonstrates its efficacy in the addressed design problems, it is advisable to examine further its applicability in more complex, higher-dimensional industrial and engineering challenges. Researchers could broaden the scope of this study to encompass technical issues characterized by multi-modal and non-linear functions with competing objectives. Additionally, further studies could involve detailed comparative analyses of this optimization method against other established algorithms to gauge its relative performance. This would provide a more comprehensive understanding of MOWSA's capabilities in a wider range of practical applications. The Matlab code for MOWSA can be obtained from <https://github.com/kanak02/MOWSA>.

## CONFLICT OF INTEREST

The authors certify that they have NO affiliations with or involvement in any organization or entity with any financial or non-financial interest in the subject matter or materials discussed in this manuscript.

## DATA AVAILABILITY

All data generated or analyzed during this study are included in this published article.

## REFERENCES

- [1] C. Renkavieski and R. S. Parpinelli, "Meta-heuristic algorithms to truss optimization: Literature mapping and application," *Exp. Syst. Appl.*, vol. 182, Nov. 2021, Art. no. 115197.
- [2] S. Kumar, G. G. Tejani, N. Pholdee, and S. Bureerat, "Multi-objective passing vehicle search algorithm for structure optimization," *Exp. Syst. Appl.*, vol. 169, May 2021, Art. no. 114511.
- [3] A. C. C. Lemonge, J. P. G. Carvalho, P. H. Hallak, and D. E. C. Vargas, "Multi-objective truss structural optimization considering natural frequencies of vibration and global stability," *Exp. Syst. Appl.*, vol. 165, Mar. 2021, Art. no. 113777.
- [4] I. Ahmadianfar, A. A. Heidari, A. H. Gandomi, X. Chu, and H. Chen, "RUN beyond the metaphor: An efficient optimization algorithm based on Runge Kutta method," *Exp. Syst. Appl.*, vol. 181, Nov. 2021, Art. no. 115079.
- [5] I. Naruei and F. Keynia, "A new optimization method based on COOT bird natural life model," *Exp. Syst. Appl.*, vol. 183, Nov. 2021, Art. no. 115352.
- [6] T. Kunakote, N. Sabangban, S. Kumar, G. G. Tejani, N. Panagant, N. Pholdee, S. Bureerat, and A. R. Yildiz, "Comparative performance of twelve metaheuristics for wind farm layout optimisation," *Arch. Comput. Methods Eng.*, vol. 29, no. 1, pp. 717–730, Jan. 2022.
- [7] S. Kumar, G. G. Tejani, N. Pholdee, S. Bureerat, and P. Mehta, "Hybrid heat transfer search and passing vehicle search optimizer for multi-objective structural optimization," *Knowl.-Based Syst.*, vol. 212, Jan. 2021, Art. no. 106556.
- [8] K. Deb and S. Gulati, "Design of truss-structures for minimum weight using genetic algorithms," *Finite Elements Anal. Design*, vol. 37, no. 5, pp. 447–465, May 2001.
- [9] L. Lamberti, "An efficient simulated annealing algorithm for design optimization of truss structures," *Comput. Struct.*, vol. 86, nos. 19–20, pp. 1936–1953, Oct. 2008.
- [10] A. K. Qin, V. L. Huang, and P. N. Suganthan, "Differential evolution algorithm with strategy adaptation for global numerical optimization," *IEEE Trans. Evol. Comput.*, vol. 13, no. 2, pp. 398–417, Apr. 2009.
- [11] H. M. Gomes, "Truss optimization with dynamic constraints using a particle swarm algorithm," *Exp. Syst. Appl.*, vol. 38, no. 1, pp. 957–968, Jan. 2011.
- [12] M. Sonmez, "Artificial bee colony algorithm for optimization of truss structures," *Appl. Soft Comput.*, vol. 11, no. 2, pp. 2406–2418, Mar. 2011.
- [13] M. Dorigo, M. Birattari, and T. Stutzle, "Ant colony optimization," *IEEE Comput. Intell. Mag.*, vol. 1, no. 4, pp. 28–39, Nov. 2006.
- [14] W. A. Bennage and A. K. Dhinra, "Optimization of truss topology using Tabu search," *Int. J. Numer. Methods Eng.*, vol. 38, no. 23, pp. 4035–4052, Dec. 1995.
- [15] G. G. Tejani, S. Kumar, and A. H. Gandomi, "Multi-objective heat transfer search algorithm for truss optimization," *Eng. Comput.*, vol. 37, no. 1, pp. 641–662, Jan. 2021.
- [16] A. H. Gandomi, S. Talatahari, X. Yang, and S. Deb, "Design optimization of truss structures using cuckoo search algorithm," *Structural Design Tall Special Buildings*, vol. 22, no. 17, pp. 1330–1349, Dec. 2013.
- [17] K. Deb, A. Pratap, S. Agarwal, and T. Meyarivan, "A fast and elitist multiobjective genetic algorithm: NSGA-II," *IEEE Trans. Evol. Comput.*, vol. 6, no. 2, pp. 182–197, Apr. 2002.
- [18] E. Zitzler, M. Laumanns, and L. Thiele, "SPEA2: Improving the strength Pareto evolutionary algorithm," *TIK-Rep.*, 2001, vol. 103, pp. 1–21.
- [19] D. W. Corne, N. R. Jerram, J. D. Knowles, and M. J. Oates, "PESA-II: Region-based selection in evolutionary multiobjective optimization," in *Proc. 3rd Annu. Conf. Genetic Evol. Comput.*, 2001, pp. 283–290.

- [20] J. Knowles and D. Corne, "The Pareto archived evolution strategy: A new baseline algorithm for Pareto multiobjective optimisation," in *Proc. Congr. Evol. Computation-CEC99*, vol. 1, 1999, pp. 98–105.
- [21] S. Kumar, G. G. Tejani, N. Pholdee, and S. Bureerat, "Improved meta-heuristics through migration-based search and an acceptance probability for truss optimization," *Asian J. Civil Eng.*, vol. 21, no. 7, pp. 1217–1237, Nov. 2020.
- [22] A. H. Gandomi and A. H. Alavi, "Krill herd: A new bio-inspired optimization algorithm," *Commun. Nonlinear Sci. Numer. Simul.*, vol. 17, no. 12, pp. 4831–4845, Dec. 2012.
- [23] E. Duman, M. Uysal, and A. F. Alkaya, "Migrating birds optimization: A new metaheuristic approach and its performance on quadratic assignment problem," *Inf. Sci.*, vol. 217, pp. 65–77, Dec. 2012.
- [24] A. Kaveh and N. Farhoudi, "A new optimization method: Dolphin echolocation," *Adv. Eng. Softw.*, vol. 59, pp. 53–70, May 2013.
- [25] C. Blum and A. Roli, "Metaheuristics in combinatorial optimization: Overview and conceptual comparison," *ACM Comput. Surveys*, vol. 35, no. 3, pp. 268–308, Sep. 2003.
- [26] M. Črepinšek, S.-H. Liu, and M. Mernik, "Exploration and exploitation in evolutionary algorithms: A survey," *ACM Comput. Surveys*, vol. 45, no. 3, pp. 1–33, Jun. 2013.
- [27] S. Mirjalili, A. H. Gandomi, S. Z. Mirjalili, S. Saremi, H. Faris, and S. M. Mirjalili, "Salp swarm algorithm: A bio-inspired optimizer for engineering design problems," *Adv. Eng. Softw.*, vol. 114, pp. 163–191, Dec. 2017.
- [28] S. Kumar, G. G. Tejani, and S. Mirjalili, "Modified symbiotic organisms search for structural optimization," *Eng. Comput.*, vol. 35, no. 4, pp. 1269–1296, Oct. 2019.
- [29] S. Mirjalili, "Moth-flame optimization algorithm: A novel nature-inspired heuristic paradigm," *Knowl.-Based Syst.*, vol. 89, pp. 228–249, Nov. 2015.
- [30] S. Kumar, G. G. Tejani, N. Pholdee, and S. Bureerat, "Multi-objective modified heat transfer search for truss optimization," *Eng. Comput.*, vol. 37, no. 4, pp. 3439–3454, Oct. 2021.
- [31] S. Mirjalili, S. M. Mirjalili, and A. Lewis, "Grey wolf optimizer," *Adv. Eng. Softw.*, vol. 69, pp. 46–61, Mar. 2014.
- [32] S. Kumar, G. G. Tejani, N. Pholdee, and S. Bureerat, "Multiobjective structural optimization using improved heat transfer search," *Knowl.-Based Syst.*, vol. 219, May 2021, Art. no. 106811.
- [33] A. Faramarzi, M. Heidarinejad, S. Mirjalili, and A. H. Gandomi, "Marine predators algorithm: A nature-inspired metaheuristic," *Expert Syst. Appl.*, vol. 152, Aug. 2020, Art. no. 113377.
- [34] S. S. Mirjalili and P. Jangir, "Multi-objective ant lion optimizer: A multi-objective optimization algorithm for solving engineering problems," *Appl. Intell.*, vol. 46, pp. 79–95, Jun. 2017.
- [35] M. Premkumar, P. Jangir, R. Sowmya, R. M. Elavarasan, and B. S. Kumar, "Enhanced chaotic Jaya algorithm for parameter estimation of photovoltaic cell/modules," *ISA Trans.*, vol. 116, pp. 139–166, Jan. 2021.
- [36] D. H. Wolpert and W. G. Macready, "No free lunch theorems for optimization," *IEEE Trans. Evol. Comput.*, vol. 1, no. 1, pp. 67–82, Apr. 1997.
- [37] A. Hertz and D. de Werra, "Using Tabu search techniques for graph coloring," *Computing*, vol. 39, no. 4, pp. 345–351, Dec. 1987.
- [38] R. Kuik, M. Salomon, L. N. Van Wassenhove, and J. Maes, "Linear programming, simulated annealing and Tabu search heuristics for lotsizing in bottleneck assembly systems," *IIE Trans.*, vol. 25, no. 1, pp. 62–72, Jan. 1993.
- [39] J.-K. Lee and Y.-D. Kim, "Search heuristics for resource constrained project scheduling," *J. Oper. Res. Soc.*, vol. 47, no. 5, pp. 678–689, May 1996.
- [40] X. S. Yang, "Review of meta-heuristics and generalised evolutionary walk algorithm," *Int. J. Bio-Inspired Comput.*, vol. 3, no. 2, p. 77, 2011.
- [41] K. Sörensen, "Metaheuristics—The metaphor exposed," *Int. Trans. Oper. Res.*, vol. 22, no. 1, pp. 3–18, Jan. 2015.
- [42] A. Kaveh and S. Talatahari, "Optimum design of skeletal structures using imperialist competitive algorithm," *Comput. Struct.*, vol. 88, nos. 21–22, pp. 1220–1229, Nov. 2010.
- [43] A. Kaveh and V. R. Mahdavi, "Colliding bodies optimization method for optimum discrete design of truss structures," *Comput. Struct.*, vol. 139, pp. 43–53, Jul. 2014.
- [44] A. Mortazavi and V. Toğan, "Sizing and layout design of truss structures under dynamic and static constraints with an integrated particle swarm optimization algorithm," *Appl. Soft Comput.*, vol. 51, pp. 239–252, Feb. 2017.
- [45] M. Farshchin, C. V. Camp, and M. Maniat, "Multi-class teaching–learning-based optimization for truss design with frequency constraints," *Eng. Struct.*, vol. 106, pp. 355–369, Jan. 2016.
- [46] S. O. Degertekin, G. Yalcin Bayar, and L. Lamberti, "Parameter free Jaya algorithm for truss sizing-layout optimization under natural frequency constraints," *Comput. Struct.*, vol. 245, Mar. 2021, Art. no. 106461.
- [47] G. Li and H. Hu, "Risk design optimization using many-objective evolutionary algorithm with application to performance-based wind engineering of tall buildings," *Structural Saf.*, vol. 48, pp. 1–14, May 2014.
- [48] C. A. Coello and A. D. Christiansen, "Multiobjective optimization of trusses using genetic algorithms," *Comput. Struct.*, vol. 75, no. 6, pp. 647–660, May 2000.
- [49] V. Mokarram and M. R. Banan, "A new PSO-based algorithm for multi-objective optimization with continuous and discrete design variables," *Structural Multidisciplinary Optim.*, vol. 57, no. 2, pp. 509–533, Feb. 2018.
- [50] G. G. Tejani, N. Pholdee, S. Bureerat, and D. Prayogo, "Multiobjective adaptive symbiotic organisms search for truss optimization problems," *Knowl.-Based Syst.*, vol. 161, pp. 398–414, Dec. 2018.
- [51] A. Kaveh and V. R. Mahdavi, "Multi-objective colliding bodies optimization algorithm for design of trusses," *J. Comput. Design Eng.*, vol. 6, no. 1, pp. 49–59, Jan. 2019.
- [52] M. Premkumar, P. Jangir, and R. Sowmya, "MOGBO: A new multi-objective gradient-based optimizer for real-world structural optimization problems," *Knowl.-Based Syst.*, vol. 218, Apr. 2021, Art. no. 106856.
- [53] A. Kaveh and M. Ilchi Ghazaan, "A new VPS-based algorithm for multi-objective optimization problems," *Eng. Comput.*, vol. 36, no. 3, pp. 1029–1040, Jul. 2020.
- [54] J.-S. Chou and D.-N. Truong, "Multiobjective forensic-based investigation algorithm for solving structural design problems," *Autom. Construction*, vol. 134, Feb. 2022, Art. no. 104084.
- [55] S. Kumar, P. Jangir, G. G. Tejani, and M. Premkumar, "MOTEO: A novel physics-based multiobjective thermal exchange optimization algorithm to design truss structures," *Knowl.-Based Syst.*, vol. 242, Apr. 2022, Art. no. 108422.
- [56] S. Kumar, P. Jangir, G. G. Tejani, and M. Premkumar, "A decomposition based multi-objective heat transfer search algorithm for structure optimization," *Knowl.-Based Syst.*, vol. 253, Oct. 2022, Art. no. 109591.
- [57] D. E. C. Vargas, A. C. C. Lemonge, H. J. C. Barbosa, and H. S. Bernardino, "Solving multi-objective structural optimization problems using GDE3 and NSGA-II with reference points," *Eng. Struct.*, vol. 239, Jul. 2021, Art. no. 112187.
- [58] J. P. G. Carvalho, É. C. R. Carvalho, D. E. C. Vargas, P. H. Hallak, B. S. L. P. Lima, and A. C. C. Lemonge, "Multi-objective optimum design of truss structures using differential evolution algorithms," *Comput. Struct.*, vol. 252, Aug. 2021, Art. no. 106544.
- [59] S. Anosri, N. Panagant, S. Bureerat, and N. Pholdee, "Success history based adaptive multi-objective differential evolution variants with an interval scheme for solving simultaneous topology, shape and sizing truss reliability optimisation," *Knowl.-Based Syst.*, vol. 253, Oct. 2022, Art. no. 109533.
- [60] A. Kaveh and A. Dadras Eslamlou, "Water strider algorithm: A new metaheuristic and applications," *Structures*, vol. 25, pp. 520–541, Jun. 2020.
- [61] P. Jangir and N. Jangir, "A new non-dominated sorting grey wolf optimizer (NS-GWO) algorithm: Development and application to solve engineering designs and economic constrained emission dispatch problem with integration of wind power," *Eng. Appl. Artif. Intell.*, vol. 72, pp. 449–467, Jun. 2018.
- [62] R. Cheng, Y. Jin, M. Olhofer, and B. Sendhoff, "Test problems for large-scale multiobjective and many-objective optimization," *IEEE Trans. Cybern.*, vol. 47, no. 12, pp. 4108–4121, Dec. 2017.
- [63] S. Mirjalili, P. Jangir, S. Z. Mirjalili, S. Saremi, and I. N. Trivedi, "Optimization of problems with multiple objectives using the multi-verse optimization algorithm," *Knowl.-Based Syst.*, vol. 134, pp. 50–71, Oct. 2017.
- [64] S. Vinodh, S. Sarangan, and S. Chandra Vinodh, "Application of fuzzy compromise solution method for fit concept selection," *Appl. Math. Model.*, vol. 38, no. 3, pp. 1052–1063, Feb. 2014.
- [65] S. Kumar, P. Jangir, G. G. Tejani, M. Premkumar, and H. H. Alhelou, "MOPGO: A new physics-based multi-objective plasma generation optimizer for solving structural optimization problems," *IEEE Access*, vol. 9, pp. 84982–85016, 2021.

- [66] C. A. C. Coello, G. T. Pulido, and M. S. Lechuga, "Handling multiple objectives with particle swarm optimization," *IEEE Trans. Evol. Comput.*, vol. 8, no. 3, pp. 256–279, Jun. 2004.
- [67] G. G. Tejani, N. Pholdee, S. Bureerat, D. Prayogo, and A. H. Gandomi, "Structural optimization using multi-objective modified adaptive symbiotic organisms search," *Expert Syst. Appl.*, vol. 125, pp. 425–441, Jul. 2019.



**KANAK KALITA** is currently a prominent Professor and a Researcher in computational engineering, acknowledged among the Top 2% of scientists, in 2023, by Elsevier-Scopus and Stanford University. With over ten years of experience, he has authored more than 80 SCI/E articles, edited more than ten book volumes, and accumulated more than 2000 citations with an H-index of 25. He has delivered more than 20 expert lectures and he serves on the editorial boards of esteemed journals, including *Scientific Reports* and *Frontiers in Mechanical Engineering*. His research interests include machine learning, fuzzy decision-making, metamodeling, process optimization, and composites. Proficient in Fortran, Python, MATLAB, and ANSYS, he has developed various codes for finite element analysis and optimization algorithms, making significant contributions to the field.



**NARAYANAN GANESH** brings a wealth of experience to his role as a Senior Associate Professor with the School of Computer Science and Engineering, Vellore Institute of Technology, Chennai, India. With a career spanning nearly two decades in teaching, training, and research, he has established himself as an authority in this field. His research interests include diverse and forward-thinking, encompassing software engineering, agile software development, prediction and optimization techniques, deep learning, image processing, and data analytics.



**RC NARAYANAN** received the M.E. and Ph.D. degrees from Anna University, Chennai, Tamil Nadu, India. He is currently an Associate Professor with the Department of Computer Science and Engineering, Sona College of Technology, Salem, Tamil Nadu, India. His research interests include information retrieval image processing, optimization techniques, data warehousing, and computation complexity problems. He is a Life Member of the Computer Society of India.



**PRADEEP JANGIR** is currently associated with the Department of Biosciences, Saveetha School of Engineering, Saveetha Institute of Medical and Technical Sciences, Chennai, India. He is internationally recognized for his advances in swarm intelligence and optimization. He has published over 90 publications with more than 2100 citations and an H-index of 24. His research interests include many-objective, robust optimization, power system engineering optimization, multi-objective optimization, swarm intelligence, evolutionary algorithms, and artificial neural networks. He is working on the application of multi-objective, many-objective, and robust meta-heuristic optimization techniques as well.



**DIEGO OLIVA** (Senior Member, IEEE) received the B.S. degree in electronics and computer engineering from the Industrial Technical Education Centre (CETI), Guadalajara, Mexico, in 2007, the M.Sc. degree in electronic engineering and computer sciences from Universidad de Guadalajara, Mexico, in 2010, and the Ph.D. degree in informatics from Universidad Complutense de Madrid, in 2015. He is currently an Associate Professor with Universidad de Guadalajara, Mexico. He has the National Researcher Rank 2 distinction by Mexican Council of Science and Technology. His research interests include evolutionary and swarm algorithms, hybridization of evolutionary and swarm algorithms, and computational intelligence.



**MARCO PÉREZ-CISNEROS** (Senior Member, IEEE) received the B.S. degree (Hons.) in electronics and communications engineering from Universidad de Guadalajara, Mexico, in 1995, the M.Sc. degree in industrial electronics from ITESO University, Guadalajara, in 2000, and the Ph.D. degree from the Institute of Science and Technology, UMIST, The University of Manchester, U.K., in 2004. Since 2005, he has been with CUCEI, Universidad de Guadalajara, where he is currently a Professor and the Rector of CUCEI. He has published over 75 indexed papers, currently holding an H-index of 17. He is the author of seven textbooks about his research interests. His current research interests include computational intelligence and evolutionary algorithms and their applications to robotics, computational vision, and automatic control. He is a member of Mexican Science Academy, Mexican National Research System (SNI), and a Senior Member of IET.

...